Medical Image Analysis 67 (2021) 101820

Contents lists available at ScienceDirect

Medical Image Analysis

journal homepage: www.elsevier.com/locate/media

Survey Paper

Surgical planning assistance in keyhole and percutaneous surgery: A systematic review

Davide Scorza[a,b,e,1,*], Sara El Hadji[b,1], Camilo Cortés[a,e], Álvaro Bertelsen[a,e], Francesco Cardinale[c], Giuseppe Baselli[b], Caroline Essert[d], Elena De Momi[b]

[a] Vicomtech Foundation, Basque Research and Technology Alliance (BRTA), Donostia-San Sebastián, Spain
[b] Department of Electronics, Information and Bioengineering (DEIB), Politecnico di Milano, Milan, Italy
[c] Claudio Munari Centre for Epilepsy and Parkinson surgery, Azienda Socio-Sanitaria Territoriale Grande Ospedale Metropolitano Niguarda (ASST GOM Niguarda), Milan, Italy
[d] ICube Laboratory, CNRS, UMR 7357, Université de Strasbourg, Strasbourg, France
[e] Biodonostia Health Research Institute, Donostia-San Sebastián, Spain

ARTICLE INFO

Article history:
Received 4 December 2019
Revised 7 August 2020
Accepted 7 September 2020
Available online 1 October 2020

MSC:
41A05
41A10
65D05
65D17

ABSTRACT

Surgical planning of percutaneous interventions has a crucial role to guarantee the success of minimally invasive surgeries. In the last decades, many methods have been proposed to reduce clinician work load related to the planning phase and to augment the information used in the definition of the optimal trajectory. In this survey, we include 113 articles related to computer assisted planning (CAP) methods and validations obtained from a systematic search on three databases. First, a general formulation of the problem is presented, independently from the surgical field involved, and the key steps involved in the development of a CAP solution are detailed. Secondly, we categorized the articles based on the main surgical applications, which have been object of study and we categorize them based on the type of assistance provided to the end-user.

Contents

* Corresponding author.
E-mail addresses: davide.scorza@polimi.it (D. Scorza), davide.scorza@polimi.it (S. El Hadji).
[1] Authors equally contributed.

https://doi.org/10.1016/j.media.2020.101820

1. Introduction

Minimally Invasive Surgeries (MIS) are commonly accepted as representing a group of surgical procedures "*associated with a lower post-operative patient morbidity compared with a conventional approach for the same operation*" (Ochsner (2000)). In general, MIS procedures present for the patient a reduced number of cuts, a faster healing time, reduced pain and bleeding after the operation, limited scarring and shorter hospitalization (Mack (2001)). Therefore, they have known a growing interest in the past decades, in the medical community but as well in the field of computer science, where the development of multiple computer-assisted techniques has seen a proportional growth.

Many MIS are performed accessing patient's body through one or more small incisions or a natural cavity and require the insertion of surgical instrumentation. In some interventions, the surgeon has the possibility to insert an endoscope, which provides a direct visual feedback of the operating scenario (e.g. laparoscopy). In case of endovascular procedures, the surgical instrumentation is inserted through a catheter, which limits the movements to the main vascular tree. Such procedures are also supported by intraoperative fluoroscopy, ultrasound imaging or tracking methods, which provide a continuous feedback to the surgeon about the catheter position.

Percutaneous keyhole surgeries (e.g. tumour ablation) and stereotactic procedures (e.g. keyhole neurosurgery) usually do not provide a clear view of the surgical scenario, and the positioning of the instruments requires to be accurately planned to guarantee an effective and safe procedure. Therefore, preoperative surgical planning has a crucial role. However, it can be complex and time consuming due to the numerous aspects that have to be taken into account. Surgeons have to accurately study the patient's anatomy and define one or more trajectories along which inserting the tool to maximize the efficacy of the intervention while ensuring the safety of the patient.

Most of existing commercial Computer Assisted Planning (CAP) solutions limit the user to an interactive definition of the trajectories by navigating the preoperative images and do not provide suggestions or quantitative information regarding the safety of the trajectory path, the access point or the target coverage.

In the recent years, different research groups have focused their efforts on the development of semi-automated or automated planners and decision support systems to assist surgeons during this phase. Fig. 1 reports the number of publications per year that focused on surgical planning assistance for percutaneous interventions and were published in the last two decades (search details are described in appendix). To the best of our knowledge, available literature reviews in keyhole surgery are mainly focused on methods to model needle-tissue interaction (Abolhassani et al. (2007)) or on specific procedures (e.g. Schumann et al. (2010b); Zhang et al. (2019) entirely focused on percutaneous liver tumour ablation). Despite the growing interest

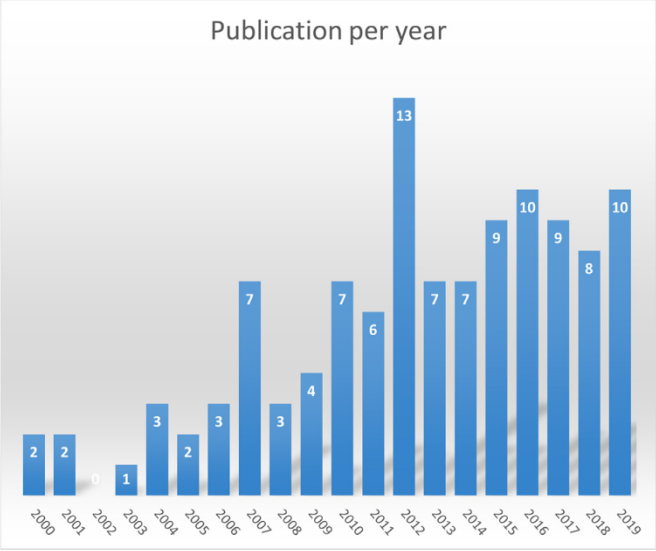

Fig. 1. Graph reporting the number of publications per year in surgical planning assistance solutions.

to this topic, a comprehensive literature review which analyzes the decision-making process of surgical planning from a methodological point of view, providing a generalization of the problem and enhancing differences and similarities of the methods proposed is still lacking.

In this work, we provide a generalized view of the surgical planning problem related to keyhole procedures and, independently from the application, we describe the necessary steps to model the intervention, the approaches used to assist the surgeon in the decision process of planning straight trajectories, and the experiments carried out to verify the clinical effectiveness (Section 2).

In Section 3, we classify the different algorithms based on the type of assistance provided to the final user, focusing on the technical aspects of their implementation.

In Section 4, we report all the clinical applications that have been object of study for the development of surgical assistance tools, describing their clinical aspects and identifying the anatomical site involved.

From our systematic search, we included a total of 113 articles related to planning assistance solutions in different keyhole surgeries.

This review is intended for researchers and engineers from universities and companies approaching the surgical planning in percutaneous surgeries. It provides a panorama on different surgical interventions, enhancing the transversality of the methods proposed in literature, which may be translated to new surgical fields. Along the article, we link the reader to additional papers regarding more specific topics, such as segmentation methods for spe-

Table 1
Common requirements for the modelling of percutaneous surgical planning interventions.

Constants	Variables	Objectives	Operators
Organs		Avoid	Distance
Tissues	EP	Reach	Angle
Functional areas	TP	Maximize	Coverage
		Minimize	

cific anatomies and optimization strategies providing technical and practical tips that can help in the development of surgical planning assistance methods.

2. General problem formulation

Planning a keyhole intervention is a complicated and time consuming task, where multiple requirements need to be considered simultaneously. Depending on the surgical application, clinicians may have to define the optimal access path to reach a target, the optimal set of parameters to perform an ablation and/or the best target point position to place an implant or to perform a biopsy. The requirements to meet safety and efficacy vary depending on the surgical intervention, the anatomical zone, and the medical workflow.

An accurate specification of the characteristics of the intervention, or clinical requirements, is the preliminary step to model the decision process that guides the planning procedure. Usually this phase requires a strict collaboration with, at least, one clinical group and to interact with surgeons with expertise in planning such interventions. Understanding the entire surgical workflow, from the preoperative image acquisition to the postoperative follow-up, can be useful to decompose the surgical procedure in different phases and provide additional information about how the procedure is performed, the hardware used and the type of imaging available.

A straight *trajectory* can be defined as a set of 3D Euclidean coordinates, corresponding to an Entry Point (EP) and a Target Point (TP) in the image space, that completely identify the path of a surgical instrument. They constitute the *variables* of the problem. The planning is the choice of the trajectory that best fits all the predefined clinical requirements. This is usually achieved using an optimization model that tries to calculate this path by translating clinical requirements into *geometric constraints* to be satisfied and optimized. A geometric constraint is the combination of constants and variables using *operators* to describe relative geometric relations between them, the *constants* being the anatomical structures of interest extracted from the preoperative images. For instance, an optimal surgical path will usually try to avoid all the dangerous structures and maximize its distance from them, to allow for sufficient space around those obstacles and account for the dimensions of the tool and possible insertion errors. The trajectory direction must also often follow other practical considerations regarding its feasibility on the considered anatomical structures, such as slippery organs boundaries or specific anatomical Regions Of Interest (ROIs) that have to be crossed a certain way. Similarly, depending on the type of application, a trajectory planning algorithm should account for the effects and characteristics of the instrument inserted. For example, in the case of percutaneous thermal ablations, the probe and TP positions are chosen based on the coverage of the targeted structure by the ablation volume. Most of the clinical requirements can be translated using a limited set of geometrical variables, constants and operators that will represent the majority of the constraints. Table 1 provides a summary of the most common ones.

Independently from the application, we can identify four main components when designing a planning assistant:

1. *Image processing*: it defines the processing of patient's preoperative images such as multimodal image registration and segmentation of relevant anatomical structures. Generally, this preliminary processing is needed to obtain the structures of interest reported in Table 1 as *constants*.
2. *Formalization*: it defines the objectives of a planning strategy and how to combine the operators, constants and variables to represent the surgical rules.
3. *Optimization strategy*: it defines the way in which the different constraints should be taken into account and how to explore the available solution space in order to reach the optimal ones.
4. *Performance metrics and experimental design*: it defines a set of experiments and the validation protocol to compare the results proposed by a planning assistant with respect to the real clinical benchmark. Depending on the maturity level of the system, different experiments can be performed to test and improve the implemented strategy.

As will be detailed in Section 3, planning assistant solutions may have different autonomy levels depending on the type of assistance provided to the user. However, the steps listed above are common for the majority of the articles reported in this review, and may be applied to different typology of CAP solutions. In the following sections we describe each component in detail, providing to the reader an overview of the methods and mathematical formulation at the base of planning assistance solutions. In Section 2.1, we provide a brief generic overview on the type of images commonly used in MIS, and focus on the image processing required to obtain the planning constants described in Table 1. In Section 2.2 we provide a formalization of the planning problem, presenting examples of typical operators and how different authors have represented a clinical requirement as a geometric constraint. In Section 2.3, we provide a formalization of the planning problem as an optimization procedure, with an overview on the strategies and methods used in literature. Finally, in Section 2.4, we classify the different types of experiments used to validate a planning assistance, enhancing their respective advantages and drawbacks.

2.1. Image processing

Acquired medical images vary according to the type of information the surgeons have to visualize, and can be categorized into two main groups: *structural imaging*, aiming to visualize the patient anatomy, and *functional (or physiological) imaging*, which measures changes in the metabolism, oxygenation, blood flow or chemical components of a target tissue. At least one structural image (usually a Computed Tomography (CT) or Magnetic Resonance Imaging (MRI)) must be acquired based on the type of tissues and organs intended to visualize. In some cases, a second acquisition with the use of contrast medium is performed to enhance additional structures (e.g. vessels) that were not visible with the normal acquisition. Especially in neurosurgery, functional imaging (mostly functional MRI (fMRI)) and Diffusion Tensor Imaging (DTI) are widely used to map the functionality and connectivity of the different brain areas. Accordingly, the segmentation of all the relevant structures, that will be used as constants, is a required step to correctly quantify the risk associated to a specific trajectory. Anatomical segmentation is a very wide topic and there are many different methods proposed in the literature which varies based on the anatomical structure and specific image modalities. Some of them are very specific for a target anatomy, while others are more generic and can be interactively used to segment a variety of structures. The description of the different segmentation methods is out of the scope of this review. Nevertheless, we provide

a generic categorization based on the interaction level required to the user:

- *manual segmentation*: the user delineates and labels the relevant structures through the use of a CAP workstation or similar software;
- *interactive segmentation*: generic algorithm where the user provides limited and simple input to segment a structure (e.g. thresholding or region growing);
- *automated methods*: pipelines of algorithms aiming to segment specific organs or structures in full autonomy. This includes for instance atlas-based methods, machine learning and deep learning techniques.

Depending on the anatomical complexity of the surgical site, a combination of those methods may be used. More detailed information is provided in Section 4.

2.2. Formalization

Once the critical or targeted structures have been identified and segmented, operators should be chosen to specify the relative position of the trajectory, e.g. the distance or the angle, the positioning or the coverage of the target. Some of them require preprocessing steps to be performed on the images.

The distance from critical structures is one of the main operators commonly considered in percutaneous interventions, determining the minimum or maximum distance at which an instrument can be placed from a critical structure. By providing a binary mask of all relevant anatomical regions, an efficient way to compute distances is through the use of distance Euclidean transform algorithms: De Momi et al. (2014) and Scorza et al. (2017a) computed a distance map volume based on the method proposed by Danielsson (1980), while Noble et al. (2010a) used a fast marching algorithm based on Sethian (1999) to compute the distance from surrounding surfaces and binary structures. Other authors (Schumann et al. (2010a, 2015)) combined different anatomical structures such as lungs, bones, cartilages and vessels into a single mask and then computed the Euclidean distance transform. Such approaches are computationally convenient since they require to compute the distance once at the beginning, with respect to a binary mask provided by the user. Similarly, Shamir et al. (2010b, 2012) used a set of distance maps to build a so-called risk volume, asking the surgeons to define a risk for each segmented structure. This approach allows to aggregate structures with the same risk in a unique mask, reducing the number of distance maps to be computed. Zelmann et al. (2015) used the distance map to provide a preferential sampling of target points around the center of the target structure. Segmented structures are commonly transformed into triangular meshes (Lorensen and Cline (1987)) to work with their surface representation. Therefore, different authors (e.g. Sparks et al. (2017b); Navkar et al. (2010); Rincón-Nigro et al. (2013)) exploited mesh properties to efficiently compute intersections and distances by the construction of bounding boxes and bounding volume hierarchies (Karras (2012)). In Wicker and Tedla (2004); Mendel et al. (2013), a more geometrical approach is computed to determine safe corridors based on specific anatomical considerations on the structure to operate (e.g. vertebras or pelvis).

The operator angle has different possible usages in trajectory planning: Scorza et al. (2017a), Sparks et al. (2017a), and Baegert et al. (2007b) computed the angle between the trajectory and the surface normal of an organ, to avoid tangential trajectories that can be too slippery; Essert et al. (2010, 2012a) computed the angle between the trajectory and the main axis of the targeted structure, to provide the correct alignment at the target point; Seitel et al. (2011) computed the angle of the trajectory with respect to one of the main anatomical planes, to ensure a good visualization during the intervention.

The target coverage indexes are generally computed as the overlapping region between two volumes. The first volume represents the targeted structure, while the second volume simulates the effect of a surgical instrument to predict its efficacy. Examples of simulated volumes are the ablation volume (Baegert et al. (2007c)), or the recording capacity of an electrode (Zelmann et al. (2015); Sparks et al. (2017b)).

Finally, the accurate positioning of a target is a fundamental requirement, which is generally influenced by all the previous variables. However, some applications as for example deep brain stimulation often uses functional data to provide additional information and define the target position of the tool inserted (D'Haese et al. (2005, 2012); Guo et al. (2007); Dergachyova et al. (2018)).

2.3. Optimization strategy

The optimization strategy is an approach to find the best values of EP and TP, based on an evaluation of the constraints and their associated objectives. Thanks to the previous formalization step, we can consider the optimization process as independent from the specific anatomy or the surgical procedure. The surgical planning process can be modeled as a constrained optimization problem, subject to a series of so-called hard (strict) and soft constraints (Essert et al. (2012b)) defined as:

- *Hard (or strict) constraints*: set of binary conditions that must be satisfied to generate the space of possible solutions (e.g. critical structure avoidance);
- *Soft constraints*: set of requirements that must be satisfied at best, usually defined by numerical cost functions (e.g. maximize the distance from vascular structures)

While hard constraints determine the available space of solutions, soft constraints guide the optimization strategy in the search for the optimum values. Depending on the complexity of the problem, it may be necessary to model it by defining one aggregative cost function (single-objective approach) or multiple independent cost functions (multi-objective approach). Some authors modelled the surgical problem by a so-called constrained single-objective optimization problem, constituted by a single cost function subject to a set of equality and inequality constraints. However, such approaches usually focus on specific parts of the whole planning problem such as the coverage at the target point (Lung et al. (2004); Deng and Liu (2007)) or distance to a critical structure (Ahmadi et al. (2009); Herghelegiu et al. (2011)).

However, in the majority of the cases, surgical trajectory planning requires to be modeled as a constrained Multi-Objective Optimization (MOO) problem, defined as:

$$\underset{x\in\Re^k}{\text{minimize}}\ \mathbf{F(x)} = [f_1(\mathbf{x}), f_2(\mathbf{x}), \ldots, f_N(\mathbf{x})]^T$$

subject to:

$$G_i(\mathbf{x}) \leq 0 \quad \text{where } i = 1, \ldots, M$$
$$H_j(\mathbf{x}) = 0 \quad \text{where } j = 1, \ldots, E$$

where $F(\boldsymbol{x})$ represents a vector of N objective functions, $G_i(\boldsymbol{x})$ and $H_j(\boldsymbol{x})$ express the set of M and E inequality and equality constraints, respectively. The vector of decision variable is $\boldsymbol{x} \in \Re^k$, where k represents the number of independent variables. Satisfying equality and inequality constraints defines the so-called *feasible design space* (or *feasible decision space* or *constraint set*) $\boldsymbol{\chi} = \{\boldsymbol{x} \mid G_i(\boldsymbol{x}) \leq 0 \text{ with } i = 1, \ldots, M \text{ and } H_j(\boldsymbol{x}) = 0 \text{ with } j = 1, \ldots, E\}$. The corresponding *feasible criterion space* (or *feasible cost space* or *attainable set*) $\boldsymbol{Z} = \{F(\boldsymbol{x}) \mid \boldsymbol{x} \in \chi\}$ determines all the possible solution points with respect to the cost func-

tions (Marler and Arora (2004)). The definition of optimal solution in MOO problems leads to the concept of *Pareto Optimality* (Vilfredo Pareto, 1906), defined as the vector of solution $\boldsymbol{a} \in \boldsymbol{\chi}$ *if* $\nexists \boldsymbol{b} \in \boldsymbol{\chi} | \boldsymbol{F(b)} \leq \boldsymbol{F(a)}$ *and* $f_i(\boldsymbol{a}) \leq f_i(\boldsymbol{b})$ for, at least, one cost function. Explicitly, Pareto optimal solutions represent all the solution vectors in the criterion space $\boldsymbol{Z}$ that cannot be improved with respect to one cost function without deteriorating the value of another cost function (*Pareto front*). Several methods were developed and studied for the exploration of the criterion space and the identification of the optimal solutions in different engineering fields (Cui et al. (2017)), and, as proposed in Marler and Arora (2004), we can identify two main categories: *scalarization methods* and *vector optimization methods*. Scalarization methods reduce the problem to a single equation, composed by the independent cost functions opportunely weighted. The most common approach in surgical planning, probably because of its simplicity and intuitiveness, is the *weighted sum method*[2], mathematically expressed as:

$$F(x) = \sum_{i=1}^{N} \omega_i * f_i(x) \tag{1}$$

with $0 \leq \omega_i \leq 1$ and $\sum_{i=1}^{N} \omega_i = 1$. The weights have to be defined *a priori*, based on the importance of each constraint. Similar techniques have been used by Schumann et al. (2010a) and Helck et al. (2016), where the authors used a *weighted product* method to combine the cost functions, or in Noble et al. (2010a) where each cost function is represented through a logarithmic scale in order to make comparable very different values.

Shamir et al. (2010a, 2012); Trope et al. (2015); De León-Cuevas et al. (2017) used a single cost function based on the distance to critical structures. However, they gave them different weights based on the suggestions of clinicians. While this technique may be very effective from a practical point of view, especially because surgeons are usually able to express the priority of each constraint, the definition of those weights may not be straightforward. The majority of the approaches define them empirically based on surgeons' suggestions and iterative experiments. Zelmann et al. (2015) used a questionnaire filled by three clinicians to define the weights and hard constraints values, while Liu et al. (2014) extrapolated them by studying iterative experiments on 10 trajectories by two surgeons and trying to identify their preference. Essert et al. (2010, 2015) presented a method for the optimal definition of weights by the analysis of retrospective Manually Planned (MP) trajectories, and reverse-engineering of the weights.

Another method to weigh multiple criteria is the *analytic hierarchy process* (Saaty (2008)), that has been used by Solitro and Amirouche (2016). The method consists in the definition of a pairwise comparison matrix, which determines the relative importance of a criterion with respect to another and is used to compute the real weights.

Scalarizing approximations, as well as single cost function problems, are usually solved by means of classical optimization approaches, that can be grouped between *gradient-based* and *gradient-free* methods (Andersson (2000)). Gradient-based methods require the analytical expression of the cost function derivative (or its approximation), which is used at each iteration to determine the search direction and explore the criterion space to reach the optimal solution. The gradient-descent method has been used in Altrogge et al. (2006), and a multi-scale version by Altrogge et al. (2007). Chen et al. (2006) used an *unconstrained steepest descent* algorithm, while Baissalov et al. (2001) used a modified version with limited memory of the Broyden-Fletcher-Goldfarb-Shanno (BFGS) algorithm.

However, since the definition of the cost-function derivative is not always straightforward, gradient-free optimization algorithms are more commonly used. Such algorithms treat the cost function as a *black-box* and implement different strategies usually based on the perturbation of their independent variables to explore the solution space. At each iteration, the cost function value is computed and the perturbation strategy updated to minimize this value. Hence, the *Nelder-Mead* algorithm (also known as *downhill simplex* or *AMOEBA*) (Nelder and Mead (1965)) has been used in Villard et al. (2005); Baegert et al. (2007c,a); Essert et al. (2010, 2012a); Xiaozhao et al. (2016); Hamzé et al. (2015); Knez et al. (2015), and the *Powell* algorithm (Powell (1964)) in Noble et al. (2010a); Butz et al. (2000). Since each algorithm implements a different optimization scheme, Villard et al. (2004) tested the previous optimization methods and the *Simulate Annealing* algorithm (Kirkpatrick et al. (1983)) and compared the results on their specific application. Jaberzadeh and Essert (2016) compared the usage of seven gradient-free optimization methods, studying their advantages and drawbacks applied to the cryosurgery ablation of liver tumours. These approaches are computationally efficient, but are sensitive to their initial position and require a suitable initialization. Many authors[3] preferred to use an *Exhaustive search* method (also called *Brute force* method), consisting in the exploration of the whole search space.

Contrary to scalarization methods, vector optimization approaches consider each cost function as independent, and try to find the optimal set of solutions lying on the Pareto front. The algorithms in this category are usually based on a *a posteriori* definition of preferences and explore the available criterion space to identify the optimal solutions lying on the Pareto front. In surgical planning domain, only few studies have explored *dominance based* optimization methods, which rely on the concept of *Pareto dominance*: a solution vector $\boldsymbol{a}$ dominates $\boldsymbol{b}$ ($a \prec b$) if $\nexists \boldsymbol{b} \in \boldsymbol{\chi} | f_i(\boldsymbol{b}) \leq f_i(\boldsymbol{a})$. In other words, we can not improve our solution without deteriorating at least one cost function. A comparison between a weighted sum method and a Pareto-based approach has been presented in Hamzé et al. (2016), showing that the latter is able to propose additional solutions that could not be found with the weighted sum approach, and that those are relevant solutions often chosen by the experts. Pareto dominance methods shows to be very effective in the case of non-convex optimization problems, where the search space can be discontinuous and contain many local minima, such as surgical planning problems. Seitel et al. (2011) proposed Pareto-optimal solutions by listing only the best trajectory for each cost function, representing the so-called *Pareto-frontier*. Schumann et al. (2015) extended this concept by locally approximating the Pareto front at different starting points through an hyperboxing Pareto-approximation method presented in Teichert (2014). A genetic algorithm approximation has been proposed in Ren et al. (2014), where the authors defined a binary expression of chromosomes to represent the planning prob-

[2] Weighted sum method: Butz et al. (2000); Baissalov et al. (2001); Ren et al. (2013); Baegert et al. (2007a); Essert et al. (2010, 2012a); Noble et al. (2010a); Bériault et al. (2011, 2012b, 2012a); Liu et al. (2012); De Momi et al. (2012, 2014); Scorza et al. (2017a, 2018); Zelmann et al. (2013, 2015); Becker et al. (2013); Liu et al. (2014); Zombori et al. (2014); Nowell et al. (2016); Sparks et al. (2017a,b); Vakharia et al. (2018a,b); Knez et al. (2018b); Altrogge et al. (2006, 2007); Hamzé et al. (2015)

[3] Exhaustive search: Wicker and Tedla (2004); Ahmadi et al. (2009); Shamir et al. (2010a); Seitel et al. (2011); Bériault et al. (2011, 2012b, 2012a); Herghelegiu et al. (2011); Lee et al. (2011b, 2012); Liu et al. (2012, 2014); De Momi et al. (2012, 2014); Mendel et al. (2013); Zelmann et al. (2013, 2015); Becker et al. (2013); Zombori et al. (2014); Trope et al. (2015); Solitro and Amirouche (2016); Ebert et al. (2016); Hamzé et al. (2016); Nowell et al. (2016); De León-Cuevas et al. (2017); Sparks et al. (2017a,b); Favaro et al. (2017); Scorza et al. (2017a, 2018); Vakharia et al. (2018a); Li et al. (2019a); Marszalik and Rączka (2019)

lem, updated based on an exponential fitness function which account for different clinical requirements.

While the majority of methods exploits optimization theory as the engine of CAP solutions, a different approach has been recently presented by Zhang et al. (2019), where the authors modeled the surgical planning problem as a Markov Decision Process (MDP) to be solved through a reinforcement learning approach. Even though they presented only preliminary results based on simulation, it may represent a different and interesting area of research for the future.

2.4. Performance metrics and experimental design

The validation of surgical planning assistance algorithms is a complex task, since there are not unique solutions or standardized performance metrics to identify the *optimal* trajectory. Actually, this definition is very subjective, based on the experience of each surgeon, the quality of available images, and the specific case that is being studied. Accordingly, there are no standardized metrics available to evaluate the performance of a surgical planning assistant.

The solutions proposed are therefore usually evaluated by two main approaches, based on the type of computed indexes:

- *Quantitative validation*: a set of relevant objective metrics are compared with respect to the minimum requirements, or with respect to manually planned (MP) trajectories. There is no need to directly involve the medical staff for this type of evaluation.
- *Qualitative validation*: one or more clinicians assess the trajectories proposed by the system, providing direct feedback on their clinical feasibility, ratings, rankings, or other subjective information.

Since in most of the cases a global and unique ground truth does not exist, the quantitative validation usually compares the value of each relevant constraint that takes a role in the optimization process with respect to its initial value or, if available, the corresponding value of a MP trajectory. However, the direct comparison of manual and proposed trajectories may be misleading, considering that the manual solution may not be the most optimal. Additionally, while this approach provides objective and reliable metrics on the algorithm performances, it assumes that the optimization model and identified cost functions are correctly modelling the problem and the segmentation of the constants is completely reliable. Consequently, a quantitative validation is not able to detect incorrect solutions with respect to additional clinical criteria which may have not been included or segmentation issues (e.g. unsegmented vascular structures or lack of accuracy).

This problem is overcome by a qualitative validation, that directly involves the final user to rate the proposed solutions on the basis of his/her experience. In this case, the user is assessing the proposal globally, and typically many different issues may arise due to sub-optimal or erroneous segmentation, missing or erroneous representation of an objective. On the other hand, qualitative validation may lack of objectivity, since there may be a high variability between surgeons regarding the definition of the "*optimal solution*" (as demonstrated in Vakharia et al. (2018b)) and the *inter* and *intra*-operator variability should be taken into account (as in Knez et al. (2018a)).

In order to perform these validations, three main categories of experimental setups can be used, depending on the type, completeness and realism of available input data:

1. *Simulations*: the algorithms are tested on synthetic data or data obtained from retrospective preoperative images (e.g. a tumour volume). However, these experiments usually lack of realism since, even if target regions and obstacles may have been obtained by clinical images, they usually test algorithms in a simplified and controlled environment, with no ground truth to compare with and where the proposed solution is directly assessed by the user;
2. *Retrospective study*: the algorithm is tested on image datasets of past cases and the results are validated with respect to the surgeon choice (being quantitative, qualitative or both);
3. *Prospective study*: the algorithm is used on new patient cases as an alternative to the traditional planning method. The solution proposed is directly assessed by the user and, if possible, compared with traditional planning methods.

Table 2 reports the articles grouped based on the validation experiments presented. Qualitative validations are also divided between single surgeons evaluation, multiple surgeons from the same institution or external raters.

The use of these different setups also often depends on the degree of readiness of the prototype, algorithms and systems that are to be tested. The readiness can be categorized following the Technology Readiness Level (TRL) scale proposed in Mankins (1995). In the current usage described in Héder (2017), the TRL scale ranges from 1 (Basic Principles Observed and Reported) to 9 (actual system proven in operational environment). Most published surgical planning assistance algorithms and tools can be considered in the 3 (experimental proof of concept) to 7 (system prototype demonstration in operational environment) range.

Simulations are usually used at the preliminary stage of the proof of concept (Table 2-a). Constraints values are computed and compared with the corresponding minimum values defined for the application (e.g. minimum acceptable distance from a vessel). The algorithms and systems tested through such experiments usually go from TRL 3 to 4.

A widely used experiment, that does not require to directly involve the medical staff, is the *retrospective quantitative* validation (TRL 4 to 5), where past cases are used to test the behaviour of the system and the trajectories planned by the clinicians represent the ground truth (Table 2-b). Because of the drawbacks of quantitative evaluation, *retrospective qualitative* studies are an alternative or complement closer to the clinical scenario, where the system is directly evaluated by one or more clinicians (TRL 4 to 6). The experimental design may vary depending on the case and the availability of the medical staff: in Becker et al. (2012); Schumann et al. (2010a); Lee et al. (2011b, 2012); Zelmann et al. (2015), a single surgeon compared the feasibility of the trajectories with respect to the clinical practice, while in Schumann et al. (2015); Bériault et al. (2011, 2012a); Trope et al. (2015); Nowell et al. (2016) multiple surgeons from the same center reviewed and evaluated the proposals. In De Momi et al. (2012, 2014); Seitel et al. (2011) the authors asked the raters to express a preference with respect to MP trajectories, comparing the proposal with the past clinical practice. Liu et al. (2012) focused the validation in understanding if the weights used in the optimization process effectively captured the clinician's preferences: after calibrating such parameters on a reduced training set, raters were asked to pick up between a MP trajectory and the one optimized by the system, blinded to their identity. Similarly, Becker et al. (2013) asked a clinician to rate trajectories coming from different sets, some manually defined by other surgeons, others automatically computed by their system. In Sparks et al. (2017b) a blind surgeon rated the trajectories proposed by their system, without knowing the origin of the plan. Most of the previous qualitative validation experiments reported also present a quantitative comparison with MP trajectories.

Liu et al. (2014) defined their validation as *pseudo-prospective* (TRL 6), since even if they used retrospective data, they planned the trajectories as if they were new patients. Two surgeons ad-

Table 2
Summary table grouping articles based on the validation experiment performed.

	Quantitative	Qualitative
Simulation	Baegert et al. (2007a, 2007b, 2007c); Baissalov et al. (2001); Belbachir et al. (2018); Chen et al. (2006); Deng and Liu (2007); Dodd et al. (2001); Favaro et al. (2017); Gao et al. (2014); Jiang et al. (2009); Kang et al. (2012); Lim et al. (2013); Liu et al. (2016); Lung et al. (2004); Marszalik and Rączka (2019); Ren et al. (2013, 2014); Tanaka et al. (2008a,b); Villard et al. (2003, 2004, 2005); Zhang et al. (2018)	/
Retrospective	Altrogge et al. (2007); Butz et al. (2000); Chen et al. (2017); De León-Cuevas et al. (2017); D'Haese et al. (2005); Ebert et al. (2016); Essert et al. (2010, 2012a, 2015); Goerres et al. (2017a); Guo et al. (2007); Hamzé et al. (2016); Han et al. (2019); Khlebnikov et al. (2011); Knez et al. (2015, 2016a, 2016b, 2018b, 2019); Li et al. (2019a); Linte et al. (2015); Marcus et al. (2019); Mendel et al. (2013); Noble et al. (2010a); Nowinski et al. (2000); Scorza et al. (2017a, 2018); Shamir et al. (2010b, 2010a, 2012); Sparks et al. (2017a); Vakharia et al. (2018a); Vijayan et al. (2019); Wimmer et al. (2014); Zelmann et al. (2013); Zhai et al. (2008); Zombori et al. (2014)	Single surgeon: Becker et al. (2012, 2013); Lee et al. (2011b, 2012); Schumann et al. (2010a); Seitel et al. (2011); Sparks et al. (2017b); Zelmann et al. (2015); Multiple surgeons: Bériault et al. (2011, 2012a); Brunenberg et al. (2007); De Momi et al. (2012, 2014); Khlebnikov et al. (2011); Liu et al. (2012); Navkar et al. (2010); Nowell et al. (2016); Schumann et al. (2013, 2012, 2015); Seitel et al. (2011); Shamir et al. (2011); Trope et al. (2015); External raters: Liu et al. (2014); Knez et al. (2018a); Vakharia et al. (2018b, 2019b)
Prospective	/	D'Haese et al. (2005); Berber (2015); Bériault et al. (2012b); Helck et al. (2016); Vakharia et al. (2019a)

justed the weights by iterative experiments on a subset of 10 trajectories, and the validation was performed by a third clinician from another institution. Using an external rater as a reviewer for the proposed solution adds information regarding the generalizability of the optimization model. Vakharia et al. (2018b) performed a qualitative validation with 5 external raters from different institutions, to which MP trajectories and optimized ones were blindly presented. It is interesting to note that this study showed that a relevant percentage of MP trajectories was considered as unfeasible by other clinicians, enhancing the fact that the surgical planning problem cannot be reduced to a unique optimal solution. Similarly, Vakharia et al. (2019b) presented solutions to blinded external raters for evaluation. In Knez et al. (2018a), two independent surgeons planned the same set of trajectories manually two times, allowing to estimate for intra and inter raters variability, and the results were compared to automatically computed trajectories.

While retrospective qualitative validations are very effective to understand the capability of the method to reflect the clinical practice, the limitation lies in their retrospective nature. During the trajectory ratings, clinicians do not usually remember the whole clinical history of the patient and usually base the evaluation only on anatomical and bio-mechanical considerations. Such bias is intrinsically avoided in a *prospective study* (TRL $\geq$ 7), were the planning assistance is used on new patients cases, considering all the clinical aspects involved and usually compared with traditional planning method. These studies need to be approved by an ethical committee, and require the medical staff to use the new system for planning future interventions and compare its benefits with respect to traditional planning methods. D'Haese et al. (2005) reported a complete study which included retrospective and prospective validation experiments. The latter has been performed on 12 patients, and the clinicians compared the proposed solution to the planned one and judged if it was acceptable or not. Berber (2015) presented a prospective study on a pilot group of 5 patients, were the surgeons directly used the proposed software to plan the surgery. Bériault et al. (2012b) demonstrated how their solution influenced the surgeon's decision making for 7 out to 8 cases, when comparing with the traditional planning method. Helck et al. (2016) included 33 patients in their study along a year and evaluated the whole workflow, including the implemented segmentation methods. The semi-automatic proposals were rated by surgeons and, if found comparable to the expert solution, an equivalent trajectory was used. Recently, Vakharia et al. (2019a) presented a prospective study for the evaluation of CAP assistance with respect to traditional manual planning. The CAP platform was used to generate automated proposals, but also to modify the trajectories when necessary to meet surgeon criteria. Manual planning was conducted in parallel, and the plan with the lowest risk score was finally implanted. Planning times were reported, showing that CAP can considerably speed up the process.

The TRLs reported here are purely indicative, however we assume that experiments closest to the clinical practice present robust and more advanced prototypes, at least at an algorithmic level.

3. Planning assistance

A planning assistance solution is designed in order to fulfil the constraints and requirements of a specific clinical application and the respective anatomical zone involved. However, most of the proposed solutions can be easily modelled to be applicable for different clinical scenarios.

In this section, we classified the articles based on the type of assistance provided to the user and the amount of information the user has to give in the initialization step ahead of the optimization process. The articles have been grouped in Table 3, following the section structure.

The methods are presented in increasing order of automation and autonomy. In Section 3.1, we provide an overview of the methods and algorithms that augment the surgical scenario by displaying additional metrics and guide the surgeon during the choice of the optimal trajectory. In Section 3.2, we present works mainly focused on the definition and optimization of the target position and the coverage of a Volume of Interest (VOI). Section 3.3 presents the algorithms that automatically define an optimal path to reach a target, focusing on the initialization method used.

3.1. Interactive planning

An interactive preoperative planning process consists in several tasks: accurately identify the most relevant target point, choose an entry point and its corresponding trajectory, verify that the chosen trajectory is as safe as possible, and that it will allow to produce an appropriate effect while avoiding side effects. Various research groups have covered those aspects and proposed from the simplest information display system to the most complex information-based decision-making assistance tool.

Table 3
Classification of planning methods based on the assistance type provided to the user.

1. Interactive planning
1.a Display of risk information:
Nowinski et al. (2000); Gerber et al. (2014); Wimmer et al. (2014); Herghelegiu et al. (2012); Klein et al. (2009); Linte et al. (2015)
1.b Effect Visualization (on target point):
Berber (2015); Golkar et al. (2018); Essert et al. (2019); Villard et al. (2003); Zhai et al. (2008)
1.c Path Identification:
Becker et al. (2012); Baegert et al. (2007b,a); Bakhshmand et al. (2017); Brunenberg et al. (2007); Gao et al. (2014); Navkar et al. (2010); Khlebnikov et al. (2011); Rincón-Nigro et al. (2013); Shamir et al. (2010b, 2011, 2012); Schumann et al. (2012, 2013, 2015); Solitro and Amirouche (2016)
2. Automated targeting
Altrogge et al. (2006, 2007); Baissalov et al. (2001); Butz et al. (2000); Chen et al. (2006); Deng and Liu (2007); D'Haese et al. (2005, 2012); Dodd et al. (2001); Guo et al. (2007); Jaberzadeh and Essert (2016); Lung et al. (2004); Ren et al. (2013); Tanaka et al. (2008a,b); Yang et al. (2010)
3. Autonomous Path Planning
3.a Automated EP definition:
Ahmadi et al. (2009); Al-Marzouqi et al. (2007); Baegert et al. (2007c); Belbachir et al. (2018); Chen et al. (2017); De León-Cuevas et al. (2017); Dergachyova et al. (2018); Ebert et al. (2016); Essert et al. (2010, 2012a, 2015); Hamzé et al. (2016); Helck et al. (2016); Herghelegiu et al. (2011); Knez et al. (2019); Li et al. (2019a); Lim et al. (2013); Liu et al. (2016); Marcus et al. (2019); Marszalik and Rączka (2019); Nowell et al. (2016); Ren et al. (2014); Schumann et al. (2010a); Seitel et al. (2011); Shamir et al. (2010a); Sparks et al. (2017a,b); Trope et al. (2015); Vakharia et al. (2018a, 2019a, 2019b); Villard et al. (2004, 2005); Yaniv et al. (2009); Zhang et al. (2018); Zombori et al. (2014)
3.b Search space reduction:
Becker et al. (2013); Bériault et al. (2011, 2012a, 2012b); Daemi et al. (2015); De Momi et al. (2012, 2014); Essert et al. (2012b); Favaro et al. (2017); Goerres et al. (2017b,a); Han et al. (2019); Jiang et al. (2009); Kang et al. (2012); Knez et al. (2015, 2016a, 2016b, 2018b, 2018a); Lee et al. (2011b, 2012); Liu et al. (2012, 2014); Mendel et al. (2013); Noble et al. (2010a); Scorza et al. (2017a, 2018); Vijayan et al. (2019); Wicker and Tedla (2004); Xiaozhao et al. (2016); Zelmann et al. (2013, 2015)

3.1.1. Display of risk information

Highly complex clinical scenarios have steered the interest of some research groups towards the optimal and advanced representation of information with the aim of facilitating the decision-making process. Such approaches do not suggest any solution autonomously, but quantitative information regarding the risk and the surrounding anatomical structures is displayed.

In 2000, Nowinski et al. (2000) proposed a pioneer planning assistant which allowed a multi-atlas visualization to define the target point, continuous navigation and mensuration. The provided tools helped the surgeons to precisely identify the target and the surrounding structures, allowing them to measure distances directly on the medical scan.

To provide relevant information about risks and facilitate the interactive search for an optimal trajectory, Gerber et al. (2014); Wimmer et al. (2014) proposed a software that displayed a real-time feedback regarding the distance from the surrounding critical structures, while the surgeon was planning the trajectory. The target point was chosen by the surgeon at the beginning and the user interactively moved the entry point over the entry surface. The software computed the predicted error along the trajectory, and showed it as a 2D model around the path as additional information. The main purpose of this approach is to help the surgeon assess the trajectories during the exploration.

Klein et al. (2009) proposed a simulation software for pedicle screw insertion for teaching purposes. The user can plan the trajectories on the patient data, and the software is able to automatically compute a set of metrics regarding the quality of pedicle screw insertion. A similar solution is presented in Linte et al. (2015).

The second one is to color-code the information. Herghelegiu et al. (2012) developed a biopsy planner for neurosurgical exploration which provided a color-coded *stability map* that identifies the possible entry regions able to reach a pre-defined target. Additionally, they included a *distance graph*, displaying the distance with respect to any critical structures along all the trajectory points.

3.1.2. Identification and display of relevant paths

However, a rapid identification of a safe and effective path is often a key requirement in many keyhole applications. Towards this end, various techniques based on access maps or lists have been proposed, with the objective of providing a rapid glance at the possible entry points and their respective qualities.

Baegert et al. (2007b) used a surface-based ray-casting technique to determine all the possible access zones on the patient's skin surface. The zones were iteratively subdivided at the borders in order to obtain a precise cartography of the possibilities.

Navkar et al. (2010) used a surface-based rendering technique to compute a series of access maps (a *Direct Impact* map, a *Proximity map* and a *Path Length* map) which were projected on the outer surface and could be used by the surgeon to identify the most feasible entry points. With the advances of technology, Rincón-Nigro et al. (2013) extended this approach by exploiting specific algorithms optimized for Graphical Processor Unit (GPU). In particular, they used acceleration spatial data structures based on bounding volume hierarchy (BVH) to efficiently represent the critical structure meshes, which provided a rapid computation of the risk access maps.

An alternative, and less binary, approach was proposed by Khlebnikov et al. (2011). They used a *crepuscular rays* analogy and implemented a voxel-based ray casting solution exploiting GPU performances to compute all available safe paths as well as dangerous paths. They provided a two steps planning system: first, they used a multi-volume rendering to provide an overview of all available paths through a 3D representation; second, they provided a 2D slice visualization for accurate planning using cutting planes on the desired orientation, with a color-coded scheme to identify the available paths.

Similarly, Schumann et al. (2012) used a direct volume rendering techniques to build a risk structure map based on a user-defined target point and the segmentation masks of critical structures. Therefore, a cube map (Greene (1986)) was used to store all the paths which intersect risky structures, consisting in six projections obtained by placing a perspective camera centered at the target point. This technique allowed to exploit high performance *shaders* developed for computer graphic purposes, that exploits GPU architecture to speed up the computation. Finally, they projected the result of the accessible paths into the 2D views navigated by the surgeon, mapping the available access points by a color-coded scheme.

With respect to the previous works, Shamir et al. (2010b, 2012) computed a risk-volume by asking the surgeons to assign a risk factor to each segmented structure, based on the expected damage in case of intersection with the clinical probe. Therefore, a risk value is assigned to each voxel based on the risk factor

and its distance from the closest structure, and all the possible access paths are computed. Each vertex of the outer surface is colored accordingly, providing the surgeon an easy way to select the optimal trajectory. When the surgeon has picked-up one, a risk map containing all relevant values is displayed and updated in real time in case of manual modification, providing a continuous quantitative feedback. During the interactive analysis of the trajectories, a geometrical model named *safety zone sleeve* is visualized and corresponds to the positioning uncertainty worst-case scenario estimated, based on localization and target errors. Shamir et al. (2011) extended the previous method by introducing an augmented reality system, which presents the quantified trajectories on a 3D physical model, allowing the surgeon to plan the trajectory in the physical space.

Similarly, a color-coded risk map for the selection of optimal EP is provided in Bakhshmand et al. (2017), where the authors used functional and structural images to estimate the eloquence damage caused by the access paths.

While all the previous works focused their assistance in augmenting the information presented to the surgeon, other methods extended the assistance to a preliminary computation of qualities, that were displayed to the user. Brunenberg et al. (2007) proposed a method which computed all available paths to reach the target based on the distance from critical structures. The list of available paths is organized based on the distance from those structure, allowing the user to filter the available trajectories based on those distances and increase the search performances. The same year, in an extension of their previous works, Baegert et al. (2007a) proposed an approach where the access zones were color-coded according to their degree of satisfaction of the different surgical constraints for abdominal interventions. An elegant solution was provided in Schumann et al. (2013), where the user defined a set of relevant variables and compute all available paths. The authors used a direct volume rendering technique to generate cylindrical projection derived by a cube map, by positioning a perspective camera at the target point. A cylindrical projection is generated for each considered parameter (insertion depth, distance from critical structures, vertical angulation and in-plane angle), and the available trajectories are presented with a parallel coordinate plot, allowing the user to filter them based on the criterion values. Schumann et al. (2015) extended the previous method by normalizing and weighting the cylindrical projection, obtaining a single map that was used to define a set of seeds to be used as initial points for optimal trajectories computations. Such seed trajectories were used to run local optimizations and returning a solution which approximates the Pareto-front, avoiding to fall in local minimum due to the non-convexity of the optimization problem. The solution set can be navigated by the use of Pareto-sliders (one for each criterion).

Gao et al. (2014) implemented a solution for access path determination based on the visibility of the target point: with respect to the previous approximation, they generate a set of grid points uniformly distributed on a sphere surface and positioned a virtual camera at each vertex, with the focal point set to the target. The results can be navigated by the use of scatter and parallel coordinates plots. A similar application is presented by Becker et al. (2012), which presented their result by color-coding the resulting trajectories, which can be interactively chosen by the surgeon. Solitro and Amirouche (2016) proposed an interactive method for pedicle screw planning, which required the surgeon to identify the pedicle sections by manually positioning two planes. Pedicles ROIs are subsequently discretized for trajectory computation, which are filtered based on computed geometrical and clinically insertion parameters. The optimal trajectories are obtained by the AHP method, and the final one is selected by the user.

3.1.3. Visualization of the effect

Other information can be relevant to select a trajectory. One good example is the prediction of the effect that will be resulting from the chosen tool position.

In Zhai et al. (2008), GPU-accelerated algorithms were used to process and visualize the ablation necrosis zone while the surgeon interactively adjusts the trajectory. The simulated necrosis zone is generated in real-time for each candidate trajectory. Berber (2015) presented an ablation system which automatically estimates the parameters needed to generate a specific ablation volume, while the trajectory is planned by the surgeon to guarantee structure avoidance and correct positioning. Villard et al. (2003) developed a simulator accounting for deformation of the ablation zone caused by surrounding vessels, and approximated the heat-sink phenomenon by stopping it in presence of large vessels. The resulting necrotic zone is represented through a deformed ellipsoid, following the vessel's shape. More recently, several works on the precise modeling of thermal ablation in the context cryoablation using GPU have been proposed, taking into account surrounding cooling structures such as vessels Golkar et al. (2018); Essert et al. (2019).

The objective of such works is to confirm that a complete ablation is possible with a particular trajectory during the trial-and-error interactive process, and that the surrounding structure will not interfere and cause incomplete destruction. Other approaches of effect simulation were used in a more automatic framework, as presented in the next section.

3.2. Automated targeting

In most of the methods mentioned above, the target point was either manually chosen by the surgeon or arbitrarily defined as the center of mass of a structure indicated by the surgeon as the target. The automatic identification of the correct target and the positioning of probes in the optimal configuration has also been an object of study, especially for thermal ablation applications. Many works have completely focused on the analysis of the target region, identifying the best configuration for probe positioning or the set of parameters aimed to create the expected ablation zone.

Some of the algorithms proposed to simulate the ablation volume through simple geometries. Butz et al. (2000) simulated the ablation zone through ellipsoidal volumes, which were used to efficiently position one or multiple probes by optimizing the coverage of the target volume, and reducing the overlapping with the surrounding healthy tissue. Similarly, Dodd et al. (2001) analyzed the overlapping of different configurations of spherical probes, by simulating with 1, 6, 14, and cylindrical simulated ablation volumes respectively. In Ren et al. (2013), first the surgeon interactively selects a set of entry points considering the avoidance of critical structure. Subsequently, based on the tumour VOI, the *branch and bound* method (integer programming) is used to first compute the minimum number of trajectories to cover the target volume, and secondly to compute the minimal number of ablation along the trajectories.

While in the previous articles the ablation zone is simulated by geometrical primitives, other solutions used the *bio-heat transfer* equation (Pennes (1948)) to model the cooling/heating effects on the surrounding tissues. The latter is used to simulate the temperature distribution in a living tissue influenced by the blood flow effects, represented as a heat sink and sources. Such equation is usually applied through a finite element model (FEM) representing the probe, which estimates the ablation effect and, subsequently, the volume of ablated tissue. Based on that, Baissalov et al. (2001) compared three different objective functions and applied a so-called Bounded and Limited memory BFGS (L-BFGS-B) method for multiple cryo-probes optimization.

Lung et al. (2004) developed an optimization algorithm based on a force field analogy, where they compute the bio-heat equation at each iteration and applied forces to the different cryo-probes to reach the correct temperature configuration at the target volume.

Altrogge et al. (2006, 2007) focused on the optimal placement of ablation probes, computing the estimated electric potential and the heat distribution at target zone and minimizing a temperature-based objective function. Tanaka et al. (2008a,b); Yang et al. (2010) developed a more mechanical approximation method to deal with the overlapping of multiple probes. They represented the elliptical ablation volumes (bubbles) for each probe, and applied a bubble-packing algorithm where van der Waals'-like forces are simulated to move these bubbles until a minimum force configuration is found.

The usage of FEM model to run the heat-transfer simulation to define the ablation zone increases the time required to run the optimization. Consequently, Chen et al. (2006) presented a more efficient solution for modelling the RFA heat transfer, without the necessity of re-meshing when the position of the probe is updated, while Jaberzadeh and Essert (2016) explored different optimization algorithms and hybrid methods to provide a precise solution in a feasible time span.

D'Haese et al. (2005, 2012) focused their work on the preoperative selection of optimal target points on a deformable atlas, which is registered to new patient's medical scans defining the target points of the procedure. The system presented is focused on DBS surgery, reporting also additional functionalities regarding target region segmentation and statistical maps of high implants efficacy. Similarly, Guo et al. (2007) used two classes of probabilistic maps to identify the most effective target point, generating a final probabilistic map by the usage of Kriging interpolation Van Beers and Kleijnen (2004).

3.3. Autonomous path planning

Most authors have tried to completely reproduce the trajectory planning problem by developing algorithms which automatically propose the optimal computed trajectory or set of trajectories to the surgeon.

Different algorithms and modalities have been proposed, some of which are able to autonomously compute the optimal path by only knowing the target point (Section 3.3.1), while others require the user to select approximated entry points or take advantage of the anatomical region knowledge (Section 3.3.2).

3.3.1. Automated EP definition

Most of the approaches that required a precise definition of target points, i.e. the coordinates of the target or a complete VOI definition, used techniques similar to the ones described in the previous sections,

Villard et al. (2004) used a voxel-based ray casting procedure to detect the surrounding structures, and optimized the number and position of multiple ablation probes based on the coverage of the target VOI. Since the algorithm is initialized by the definition of the tumour VOI and the outer surface, Villard et al. (2005); Baegert et al. (2007c) computed and stored all the accessible paths into cube maps to reduce the possible search space, while Baegert et al. (2007a) applied the surface-based rendering algorithm presented in Baegert et al. (2007b). In particular, Baegert et al. (2007c) did not consider only one point inside the VOI as the target, but they computed the cube maps at each voxel on the VOI boundary in order to define the accessible paths. After removing non-reachable solutions, they optimized the trajectory to maximize the coverage of tumour volume while reducing the ablation of surrounding healthy tissues. Since they applied a numerical optimization strategy by the use of *Nelder Mead* algorithm, a semi-exhaustive initialization algorithm identifies all the available connected zones on the outer surface as starting points for the optimization.

Herghelegiu et al. (2011) presented an automated version of Herghelegiu et al. (2012), where the algorithm defined the available paths with the use of a stability map and suggested the best trajectory by ranking them on the base of the distance from critical structures. Similarly, Ahmadi et al. (2009) implemented a system which uniformly distributed 40 thousands points on the outer surface and defined the optimal trajectory based only on a distance from vessels criterion.

Seitel et al. (2011) used the Z-buffering algorithm implemented in computer graphics by placing a perspective camera at the center of the tumour VOI to determine the accessible entry zone by deleting the outer surface vertices occluded by surrounding structures. Subsequently, soft constraints regarding the trajectory length, the distance from critical structures and the insertion angle are computed and a Pareto-based optimization scheme is applied to determine Pareto-optimal solutions. Similar approaches were used for Deep Brain Stimulation (DBS) (Section 4.1) application by Essert et al. (2012a), where they reduced the search space entry zones by the exploitation of GPU rendering algorithm, generating cube maps view from the target point. Essert et al. (2010, 2012a) deeply analyzed the rules guiding DBS intervention and developed a generic approach based on a meta-language for the translation of such rules into geometrical constraints. While the previous works were based only on structural and anatomical constraints, Dergachyova et al. (2018) extended such methods to account for *anatomo-clinical* atlases for the selection of the optimal target point.

Schumann et al. (2010a); Helck et al. (2016) computed cylindrical projections to build different maps according to the criterion considered, which were merged to a weighted product computing directly hard and soft constraints, ranking the available trajectories. GPU architecture has been exploited also in the development of Epinav (Zombori et al. (2014); Sparks et al. (2017b)), a StereoElectroEncephaloGraphy (SEEG) (Section 4.1) automated planner which used BVH organization for the computation of intersection and distances with respect to critical structure surfaces and requires only the definition of the TPs. The GPU acceleration allows the usage of an exhaustive search method and to efficiently remove unfeasible EPs for each trajectory, based on the hard constraints provided. In Sparks et al. (2017a), the authors extended their initialization method by introducing a user-defined choice of a spatial prior inside the target region. In Vakharia et al. (2018a), the previous algorithm was used for the ablation planning of specific target zones (amygdalohippocampal complex), modelling the ablation zone by a trajectory dilation of 15 mm but limiting the entry region by suggestion of expert clinicians. A machine learning approach for studying the optimal parameters, including entry and target zones, is presented in Li et al. (2019a).

As in the interactive planning section, other authors implemented their algorithms without exploiting rendering techniques or GPU architectures. Yaniv et al. (2009) presented a multi-purpose system based on the Image Guided Surgery Toolkit (IGSTK), where they developed also an automated planning algorithm for tumour ablation in the lung. The whole pleura surface is used as initial entry region, and the number of trajectories and ablation is optimized by a branch and bound method as in Ren et al. (2013). Ebert et al. (2016) implemented an automated planning software for post-mortem robotic biopsy applications, where multiple trajectories are planned serially to reach different targets. The search space is reduced by the application of hard constraints regarding the occlusion by bony structures, and the optimization is based on the end-effector angle to reach the target. Liu et al. (2016) introduce in their work the "*collision-free reachable*

workspace", where the optimization method to find optimal trajectories takes into account the workspace of the robot used by including it kinematics in the computation. A similar work is proposed in Belbachir et al. (2018), where the available search space is defined on the whole patient skin, taking into account only the points that were reachable by the robot.

Shamir et al. (2010a) implemented an automated version which ranked the trajectory incrementally based on the risk score. As in the interactive versions (Shamir et al. (2010b, 2012)), they computed a risk volume based on the risk assigned by the surgeon to each critical structure and, for each computed trajectory, they presented a risk card reporting additional information. In a following publication, Trope et al. (2015) studied the efficacy of the automatic method with respect a traditional planning and an augmented version of their software. The same risk volume computation has been exploited by De León-Cuevas et al. (2017), which introduced the usage of fuzzy logic to better transmit to the surgeon the associate risk of a trajectory.

Lim et al. (2013); Ren et al. (2014) used a Genetic Algorithm to compute the optimal trajectories for ablation procedures. They implemented a fitness function based on the number of trajectories, the number of ablation spheres, the tumour coverage and surrounding structures which identify the optimal paths to reach the targets. The user is able to modify a set of coefficients which guide the importance of each constraint by a specific cost function.

3.3.2. Search space reduction

While the previous algorithms automatically explored the whole search space with respect to the defined target, Bériault et al. (2011, 2012a, 2012b); Zelmann et al. (2013, 2015); Liu et al. (2012, 2014) defined a set of entry regions on an atlas head surface, in accordance with the DBS intervention standards. Therefore, they registered the atlas to the new patient scan, reducing the available entry zone to the one previously defined. De Momi et al. (2012, 2014); Scorza et al. (2017a) implemented an automated planning algorithm for SEEG in which the surgeon roughly initialized each trajectory by placing entry and target points. Such points were used to generate initial entry and target search space for each trajectory, and the reduced search space allowed the usage of an exhaustive search method in a feasible time. Using a similar approach, Favaro et al. (2017) implemented a proof-of-concept automated planner for straight trajectories tested on a sheep brain scan. The algorithm presented by Noble et al. (2010a) required a manual initialization of entry and target points, or they could alternatively be estimated by an atlas registration procedure as in Al-Marzouqi et al. (2007). The method presented by Becker et al. (2013) implemented a multiport automated planner for skull-base applications that optimized the set of the three best trajectories to reach a predefined target. Again, the clinician had to roughly select a set of obvious initial candidate entry points. Some of these techniques implied a small interaction of the user and a decreased autonomy of the system, but they provide high-quality initial guesses for the optimization procedure and, at the same time, reduce the computational time.

A very different approach was applied by Kang et al. (2012) for bone tumor ablation, where the authors presented a system able to construct a statistical patient atlas registered through a deformable 2D-3D registration method to build the patient specific model. Therefore, they were able to optimize the ablation plan based on a tumor coverage criterion.

Automated planning algorithms focused on screw insertion were strictly bounded to the anatomical characteristics of the surgical site. The majority of the related articles were focused on the spine and required a characterization of the pedicular regions to run the optimization and find the optimal implant size and orientation. Wicker and Tedla (2004) applied a set of geometric assumptions to extract anatomical information from the segmented patient images. By correctly orienting each vertebra, they scanned each slice along the anterior-posterior direction looking for chords identifying four intersections defining the pedicle regions. Once the pedicles were identified, the authors could estimate the minimum pedicle width by simply computing the Euclidean distance between intersected points, and build a set of 3D coordinates as the mean points along the pedicle. Finally those points were fitted by a least square algorithm to identify the trajectory. Lee et al. (2011b, 2012) also used a set of geometrical considerations by computing vertebra symmetry axis and planes, but their method provided the definition of an optimal trajectory by imposing a safe margin with respect to the pedicle boundaries and maximized the insertion depth to improve the so-called fastening strength between the screw and vertebra interface (Krag et al. (1988)). The use of symmetry planes also allowed to avoid collisions between screws of the same vertebra. Daemi et al. (2015) developed an algorithm which considered similar constraints, linking the fastening strength to the trajectory length. Xiaozhao et al. (2016) also used a set of geometric considerations with respect to the anatomical vertebra planes, and searched for the optimal solution by maximizing the fastening strength computed at the screw boundaries. Knez et al. (2015, 2016a) based the planning of screw on the parametric modeling of pedicles as previously mentioned in Section 4.3. The screw is modeled as a cylinder positioned to cross the mid-coronal plane of the pedicle and its position is optimized with respect to the axial and sagittal angles. Trajectory and size of the final screw are estimated taking into account the 3D vertebra and pedicle models previously obtained, and maximizing the fastening strength based on the image intensities underlying the screw boundaries (similar as in Xiaozhao et al. (2016)). Knez et al. (2018b) modified the computation of the fastening strength to include additional clinical parameters, aggregated through a weighted sum approach, related to the spine curvature and following the guidelines of the most commonly used straight-forward insertion technique (Lehman Jr et al. (2003)).

Mendel et al. (2013) used a similar method for the estimation of sacro-iliac screws, which analyzed the voxel-intensity sequence by scanning a correctly oriented CT scan, and defined the maximum screw width and the optimal trajectory.

While all the previous algorithms focused on the optimization of trajectories based on anatomical constraints, in the last years other approaches tried to approximate solutions by introducing additional knowledge based on the analysis of past cases. For both spinal (Goerres et al. (2017a); Vijayan et al. (2019)) and pelvis screw (Goerres et al. (2017b); Han et al. (2019)) placement applications, the authors proposed planning methods based on the construction of a statistical shape model containing trajectory annotations. The atlas is constructed from different segmented datasets, containing annotation of expert clinicians regarding screw trajectories. An active shape model registration method is used to register a new CT volume without requiring any previous segmentation, and the optimal trajectory is computed. Following a similar idea, Scorza et al. (2018) proposed a method for the analysis of retrospective trajectories, and their accumulation in an average brain space based on their spatial position and the anatomical regions crossed. The latter focused on SEEG surgical practice, and the trajectory atlas is shown to be helpful in the initialization of optimization algorithms (e.g. Scorza et al. (2017a)). Atlas based methods represent an alternative approximation to surgical planning problems, based on the idea of encapsulating expert knowledge which may contain additional consideration rather than only anatomical or bio-mechanical constraints.

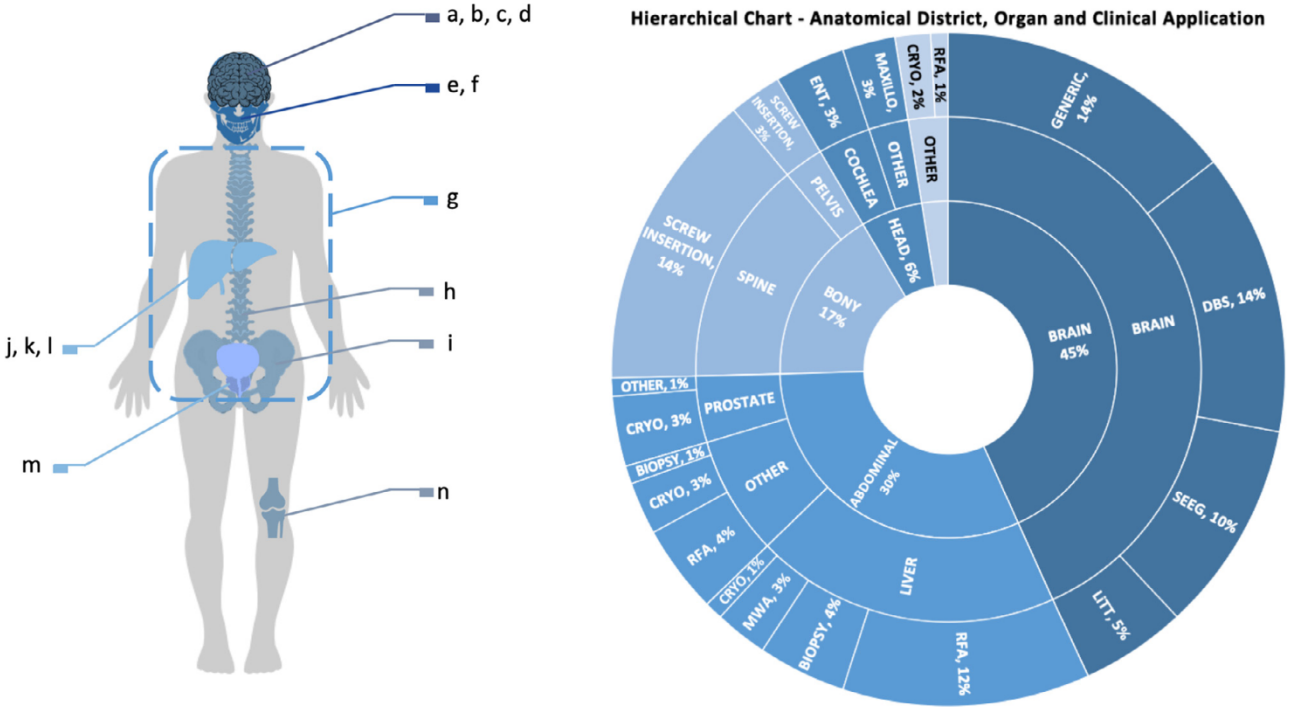

Fig. 2. The figure reports the articles found by the systematic search, associated to the anatomical district and the application described. On the right, the pie-charts presents the distribution of our results with respect to the anatomical district, the organ and the intervention.
[a] Biopsy: Ahmadi et al. (2009); Bakhshmand et al. (2017); De León-Cuevas et al. (2017); Favaro et al. (2017); Herghelegiu et al. (2011, 2012); Marcus et al. (2019); Marszalik and Rączka (2019); Navkar et al. (2010); Nowinski et al. (2000); Rincón-Nigro et al. (2013); Shamir et al. (2010a, 2010b, 2011, 2012); Trope et al. (2015)
[b] DBS: Bériault et al. (2011, 2012b, 2012a); Brunenberg et al. (2007); Dergachyova et al. (2018); D'Haese et al. (2005, 2012); Essert et al. (2010, 2012a, 2012b, 2015); Guo et al. (2007); Hamzé et al. (2015, 2016); Liu et al. (2012, 2014)
[c] SEEG: De Momi et al. (2012, 2014); Scorza et al. (2017a, 2018); Nowell et al. (2016); Sparks et al. (2017a,b); Vakharia et al. (2018b, 2019a); Zelmann et al. (2013, 2015); Zombori et al. (2014)
[d] LiTT or other type of ablation: Li et al. (2019a); Vakharia et al. (2018a, 2019b)
[e] ENT: Al-Marzouqi et al. (2007); Gerber et al. (2014); Noble et al. (2010a); Wimmer et al. (2014)
[f] Maxillo: Becker et al. (2012, 2013); Gao et al. (2014)
[g] Generic - Ablation: Butz et al. (2000); Ebert et al. (2016); Khlebnikov et al. (2011); Lim et al. (2013); Ren et al. (2013, 2014); Yaniv et al. (2009) CRYO: Essert et al. (2019); Golkar et al. (2018)
[h] SP: Daemi et al. (2015); Goerres et al. (2017a); Klein et al. (2009); Knez et al. (2015, 2016a, 2016b, 2018a, 2018b, 2019); Lee et al. (2011b, 2012); Linte et al. (2015); Solitro and Amirouche (2016); Vijayan et al. (2019); Wicker and Tedla (2004); Xiaozhao et al. (2016); Zhang et al. (2018)
[i] SP: Goerres et al. (2017b); Han et al. (2019); Mendel et al. (2013)
[j] Biopsy: Belbachir et al. (2018); Helck et al. (2016); Schumann et al. (2010a, 2012, 2013)
[k] RFA: Altrogge et al. (2006, 2007); Baegert et al. (2007c, 2007a, 2007b); Chen et al. (2006, 2017); Dodd et al. (2001); Schumann et al. (2015); Seitel et al. (2011); Villard et al. (2003, 2004, 2005); Yang et al. (2010)
[l] MWA/CRYO: Berber (2015); Jaberzadeh and Essert (2016); Liu et al. (2016); Zhai et al. (2008)
[m] CRYO: Baissalov et al. (2001); Lung et al. (2004); Tanaka et al. (2008a,b) OTHER: Jiang et al. (2009); Deng and Liu (2007)
[n] Bone ablation: Kang et al. (2012).

4. Clinical applications

Our systematic search revealed that various clinical applications have been subjects of study in the development of trajectory planning assistance systems for the percutaneous insertion of one or more needle-shaped instruments. All the articles included in the review have been classified "*per application*" and "*per anatomical district*". A schematic representation of the classification is reported on Fig. 2. Almost 45% of the works have been focusing on neurosurgical applications, distributed into Deep Brain Stimulation (DBS, 14%), StereoElectroEncephaloGraphy (SEEG, 10%), or generic interventions such as biopsies (15%) and Laser interstitial Thermal Treatments (LiTT, 4%) focused on the ablation of specific brain zones or tumoral masses. Abdominal procedures represent almost 30% of the articles found, the majority being hepatic interventions (20%). Most of them are related to tissue ablation techniques, representing almost 32% of the articles, and divided between Radio-Frequency Ablation (RFA, 17%), Cryoablation (CRYO, 7%), Microwave ablation (MWA, 3%) and LiTT (4%). Screw placement (SP, 18%) papers focus on the percutaneous insertion of screws into a bony structure, which could be potentially located everywhere in the body. However, the majority of them addresses the problem of vertebral fixation for spinal fusion, and only a few articles (Mendel et al. (2013); Goerres et al. (2017b); Han et al. (2019)) are on pelvis screw placement applications. Finally, the systematic search revealed some interesting works regarding Maxillo and ENT surgery (6%), for the safe access of internal parts of the ear or skull-base puncture for biopsies.

While each surgical application has its own requirements, in Table 4 we formalize them following the taxonomy reported in Table 1, Section 2. As expected, the variability relies mostly on the constants (the relevant anatomical structures), and how they are considered in the surgical process. Objectives and operators are usually the same, combined differently with the relevant organs and tissues to match the specific applications requirements.

In the next sections, we provide an overview of the main identified clinical applications. In particular, for each application we report a brief description of the clinical requirements to be considered for the development of an advanced CAP system, as well as

Table 4
We report the main applications found, organized based on the requirements presented in Section 2. Constants, operators and objectives may not apply to all the articles, but represent the most common requirements for each application.

			Neuro		Bony	Abdominal	Head
			Keyhole	DBS	SEEG	Spine	Keyhole and Ablation	Maxillo-ENT
Objectives - *Operators*	Constants		Brain, Skull/Skin, Vessels, Sulci, Ventricles, functional cortex and brain parcellation					
			Tumour	Amigdala, Globus Pallidus (GPi), Subthalamhic Nucleus (STN)	Gray matter, Hippocampus, Amygdala, Insula, Other electrodes	Vertebra Body, Vertebra Pedicle, Cortical Bone, Other screw	Ribs, Spine, Liver, Spleen, Tumour, Vessels	Cochlea, facial nerve, external auditory canal, ossicles
		Variables	EP; TP			EP; TP	EP; TP ; Ablation volume	EP, TP
	Avoid		Vessels, Ventricles, Sulci functional cortex	/	Other electrodes	Pedicle and Vertebra body boundaries	Vessels, Ribs	Ossicles, facial nerve, external auditory canal
	Reach		Tumour	Amigdala, GPi, STN	functional cortex	/	Tumour	Cochlea
			Distance from vessels, sulci					
	Maximize		Tumour *coverage*	functional *coverage*	GM *coverage*	Cortical bone *coverage*; Trajectory *length*	Tumour *coverage*	/
			Angle to skull/skin normal, Trajectory *length*			/		
	Minimize		*Angle* to tumour axis	/	/	/	Healthy tissue *coverage*; *Angle* to tumour axis; Trajectory *length*	/

the segmentation methods used by the authors to account for the surrounding anatomical structures.

4.1. Neurosurgery

Several neurological disorders, such as Parkinson's disease, epilepsy or tumors, happen to be resistant to drug therapy and thus require to be approached surgically through minimally invasive procedures for advanced investigation, e.g. biopsy and diagnosis, or treatment. These procedures are not trivial as they require precise targeting of lesions or anatomical landmarks with a probe or a needle inside the brain. An incorrect positioning of the surgical tool can result in severely harmful neurological complications, e.g. ineffective treatment, intracranial hemorrhage, temporary or permanent neurological deficit. Hence, they require an intensive pre-operative planning to identify specific critical structures to avoid and/or to target.

We identified three major types of neurosurgical applications that use preoperative CAP: (1) DBS, that requires the implantation of electrodes to release electrical impulses in specific brain regions, generally called deep brain nuclei, and reduce the symptoms due to movement disorders, e.g. Parkinson's Disease; (2) SEEG, which consists in implanting several multi-lead intra-cerebral electrodes recording electrical signals in order to identify the epileptogenic zone of the brain that requires to be surgically resected (Talairach and Bancaud (1973)); and (3) biopsy or generic stereotactic techniques that require the insertion of a needle-shaped instrument for tumor/lesion histological analysis or ablation. Fig. 3 presents an example of DBS (left) and SEEG (right) implant sites, with the main anatomical regions to be considered.

Considering the main objective of the above mentioned applications, it is possible to highlight some differences which also influence the constraints that must be fulfilled. DBS aims at targeting a specific anatomical structure: a key requirement to guarantee the efficacy of the treatment is the optimal selection of the stimulation point. In fact, according to different studies, the symptom improvement strongly depends on how accurately the stimulated brain area is targeted (Maks et al. (2009); Tisch et al. (2007); Herzog et al. (2004); Saint-Cyr et al. (2002)). Changing the location of the active contact within or around the nucleus may provide different positive or negative clinical outcomes. The signal coverage of some brain tissues can even cause severe side effects (Mikos et al. (2011)). Based on this observation, the solutions provided by D'Haese et al. (2005, 2012); Guo et al. (2007); Dergachyova et al. (2018) used functional data to optimize the target positioning of the inserted tool. Moreover, the anatomical structures to be targeted are only a few millimeters long, which makes targeting accuracy even more crucial. Other structures such as thalamus, amygdala or hippocampus can be used as an electrophysiological landmark when targeting, for example, the subthalamic nucleus (STN) and thus require to be segmented.

In SEEG, the goal of intracerebral electrode implantation is to maximally record EEG from a given volume. Electrode arrangements are planned in order to both maximize cortical coverage and pass through safe, avascular planes. For example, in case of mesial temporal lobe epilepsy, which is the most common type of refractory epilepsy, the main suspected regions are hippocampus (HC), the amygdala (AG) or the temporal neocortex. Therefore, it is important to guarantee not only the accurate recording from deep structures, but also a good coverage of the surrounding cortical regions. This could be obtained by ensuring electrodes pass through the maximal amount of gray matter (GM), since it is generally the component of brain tissue that generates seizures (Zelmann et al. (2015)). SEEG is also the only neurosurgical procedure that requires the planning of multiple electrodes simultaneously, which increases the algorithm complexity

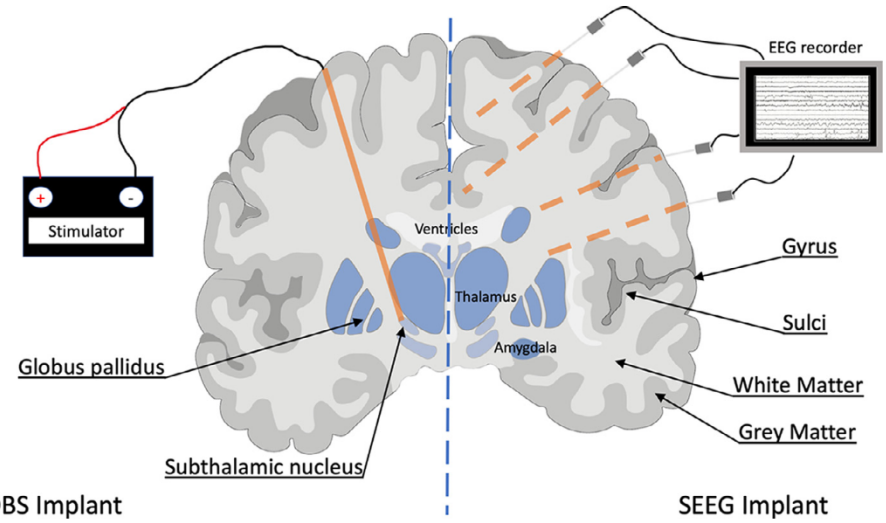

Fig. 3. Example of DBS (left) and SEEG (right) implants. DBS usually requires the implant of an electrode connected to a stimulation device for the electrical inhibition of specific brain zones such as the *subthalamic nucleus* or the *globus pallidus*. On the contrary, SEEG requires to implant multiple intra-cerebral electrodes, aiming at recording the electrical activity of different cortical and deep-located regions. Insertion EPs are commonly located on gyri, while sulci zones are avoided.

and requires specific solution to manage different possible combinations of trajectories (De Momi et al. (2014); Scorza et al. (2017a); Sparks et al. (2017b)). Nonetheless, CAPs solutions for SEEG are mostly fully automated, reducing as much as possible the interaction with the user and trying to directly propose a set of optimal trajectories.

Precise targeting of a lesion or tumour is also a fundamental requirement for biopsies and general stereotactic neurosurgical procedures, but on the other hand these applications demand a careful assessment of the functionality of the tissue surrounding the target. Mapping the brain activity and connectivity around the targeted lesion can reduce the likelihood of adverse outcomes of the stereotactic procedure. To this end, no-go zones could be defined to avoid severe cognitive, perceptual, motor, or language deficits by including and processing multiple brain imaging modalities (e.g. fMRI and DTI), as proposed by Bakhshmand et al. (2017); Trope et al. (2015); Ahmadi et al. (2009). Biopsy applications usually require the planning of a single or reduced number of trajectories, the TP could be located in very different brain regions and the surgical tool is usually more invasive than, for example, SEEG electrodes. Therefore, many authors[4] proposed an interactive assistance type, augmenting the information provided to the surgeon without directly propose an optimal trajectory.

In general, all the previously described procedures share also other common constraints and requirements that guarantee the safety of the procedure. In particular, some anatomical structures must be avoided, such as:

- *vessels*, to avoid intracranial bleeding;
- *ventricles*, to prevent leakage of cerebrospinal fluid (CSF);
- *sulci*, to decrease the probability of hitting vessels, as they can be located at any depth within a sulcus.

One of the major risks related to these procedures is intracranial hemorrhage (Benabid et al. (2009); Mullin et al. (2016); Li et al. (2019b)). To prevent that risk, 3D visualization and assessment of the cerebrovascular tree play an important role. In general, vessel segmentation methods can be divided into four categories: vessel enhancement, machine learning, deformable models, and tracking methods (Moccia et al. (2018)). Manual, semi-automatic and fully automated thresholding approaches are the most widely used methods when angiography data are available[5]. Otherwise, vessel enhancement filters are also popular approaches[6]. Sparks et al. (2017a,b); Nowell et al. (2016) integrated in their CAP solution a multi-scale, multi-modal tensor voting algorithm proposed by Zuluaga et al. (2015). Shamir et al. (2011) used an Expectation Maximization algorithm initialized by thresholding and post-processed by multi-scale vesselness filter (Frangi et al. (1998)) applied to Magnetic Resonance Angiography (MRA). Level set is then applied for vessel boundary extraction. Scorza et al. (2017b) proposed a 2D automatic vessel segmentation based on Gaussian mixture model (GMM) and Markov random field (MRF) that can be applied directly to the Maximum Intensisty Projection (MIP) image, in order to identify only vessels around the electrode. Trope et al. (2015); Shamir et al. (2012) employed the method proposed by Freiman et al. (2012), which combines an automatic watershed-based method for large vessel segmentation, and a graph-based method for small vessel segmentation and post-processing. It exploits an edge weighting function that adaptively couples the voxel intensity, an intensity prior, and a local vesselness shape prior.

Structural brain segmentation has a large literature and many different algorithms and software have been released for the analysis of MRI images. As a consequence, some of them have been used to generate the required brain structures that must be considered during surgical planning. Bériault et al. (2012b, 2011, 2012a); Zelmann et al. (2013) used a set of different algorithms based on probabilistic and multiple templates based segmentation (Collins et al. (1999, 1995, 1994)) for the identification of left and right caudate, cortical GM, ventricles and sulci. FreeSurfer (FS) is another well-known open source software tool the analysis and processing of brain images (Fischl (2012)). It offers different functionalities for image registration, skull stripping, cortical surface reconstruction and anatomical labelling among others (Fischl et al. (2002)). The results of the FS pipeline have been used as inputs for the automated planning algorithms in De Momi et al. (2012, 2014); Scorza et al. (2017a, 2018); Sparks et al. (2017b). Essert et al. (2012b) used FS specifically for the volumetric segmentation of the ventricular system, while

[4] Shamir et al. (2010b, 2010a, 2012); Navkar et al. (2010); Rincón-Nigro et al. (2013); Bakhshmand et al. (2017); Herghelegiu et al. (2011)

[5] De León-Cuevas et al. (2017); Liu et al. (2014, 2012); De Momi et al. (2012, 2014); Scorza et al. (2017a); Herghelegiu et al. (2011, 2012); Navkar et al. (2010)

[6] Zelmann et al. (2015, 2013); Bériault et al. (2012a, 2012b, 2011); Brunenberg et al. (2007); Ahmadi et al. (2009)

the scalp and cortical sulci were automatically segmented by through BrainVISA (Rivière et al. (2009)) anatomical segmentation pipeline (Mangin et al. (2004)). In Essert et al. (2012a) the cortical sulci were automatically segmented using an algorithm based on curvature information (Le Goualher et al. (1997)).

In Sparks et al. (2017b,a); Nowell et al. (2016); Vakharia et al. (2018b,a); Li et al. (2019a), Geodesic Information Flows (GIF) presented by Cardoso et al. (2015) is used to perform brain parcellation using the Brain Collaborative Open Labeling Online Resource (Brain-COLOR) atlas (Klein and Tourville (2012)) and define the anatomical labels of the cortex, GM and sulci. The brain atlas contains 142 possible regions. In Dergachyova et al. (2018); Essert et al. (2015); Hamzé et al. (2015), the preprocessing of the images was performed using the pyDBS pipeline, a fully-integrated and automatic image-processing workflow for planning and postoperative assessment of DBS interventions as described in D'Albis et al. (2015). pyDBS includes denoising, bias correction on MRI, CT image registration to preoperative MRI, automatic segmentation and 3D mesh reconstructions. In particular, after an interactive localization of the Anterior Commissure (AC) and Posterior Commissure (PC), which are essential anatomical landmarks, the pipeline performs an intensity-based segmentation of the scalp, brain, and cortical sulci, as well as an atlas-based segmentation of the brain ventricles and basal ganglia.

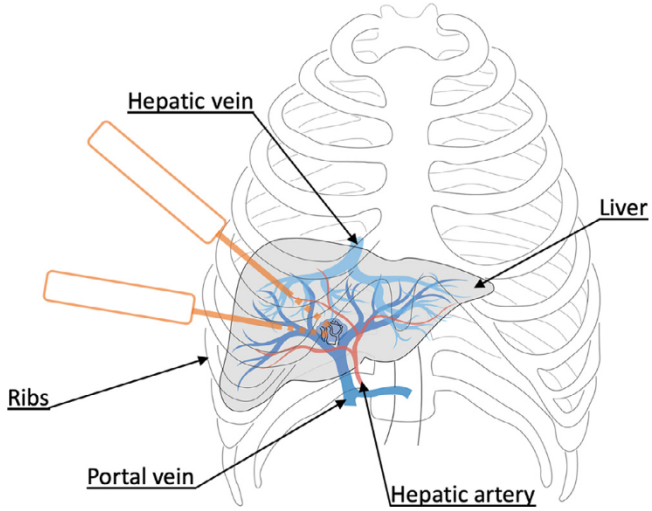

Fig. 4. Example of liver percutaneous needle insertion. The main vascular trees corresponding to the hepatic vessels are represented. In the case of biopsy, a single trajectory should be planned to reach the tumour region, avoiding ribs and vessels. In the case of an ablation procedure, depending on the tumour size, it could be necessary to plan more than a single path to guarantee the complete of ablation of the targeted volume.

4.2. Abdominal surgery and ablation techniques

The placement of needle-shaped instruments in a minimally invasive image-guided framework is a typical intervention performed in the abdominal region, e.g. liver, kidney, or prostate, for biopsies or minimally invasive tumor therapies. Percutaneous tissue ablation procedures are widely used for the local treatment of primary and metastatic tumors. These procedures aim to destroy the pathological tissue by creating a necrotic zone in the target area. The pre-operative planning of the intervention consists in finding an optimal path that guarantees both the complete ablation of the target volume and a minimum amount of affected healthy tissue and damage to adjacent vital structures.

Tissue ablation procedures might require one or more ablations to be planned in order to guarantee that the target volume is completely destroyed. In fact an incomplete ablation might increase the risk of tumor recurrence. The two major causes which can hinder a complete ablation are the following: i) difficulty in reaching the entire target volume due to technological constraints and ii) difficulty in releasing efficiently the ablative effect to the entire targeted region because of the perfusion of nearby vessels and capillary level microperfusion which interferes with the ablative effect. The articles reported in Table 3-1.b focus mainly on the simulation of the ablation zone, considering the surrounding anatomy. On the other hand, the ablative effect could affect unforeseen locations, leading to unwanted ablation of healthy tissue. Hence, an ablation procedure is considered successful if the whole target volume and the additional safety margin are covered by the coagulation and overtreatment is minimized.

In this review we considered only energy-based ablation mechanisms in which the ablation instrument is used to destroy the tissue in the target volume by changing the temperature within that region. Hyperthermic ablation, such as RFA and MWA, heats up the target region and causes an acute coagulative necrosis. The first technology uses alternating current of radiofrequency waves flowing from the electrode tip through the surrounding tissue, while MWA uses electromagnetic waves to implement thermal ablation. Within the electromagnetic field, polar molecules such as water continuously realign to the continuously changing waves. This oscillating movement generates the heating effect. All tissue within the electromagnetic field is heated simultaneously, which reduces treatment times in comparison to RFA (Huang et al. (2014); Yu et al. (2011); Gravante et al. (2008); Martin et al. (2010); Yushkevich et al. (2006)). Hypothermic ablation cools the target tissue which leads to the breakdown of cellular metabolism, formation of ice crystals and osmotic shock. Cryoablation, also referred to as cryosurgery, is the only hypothermic modality. It utilizes percutaneously placed instruments called cryoprobes to decrease drastically the temperature in the target region in order to achieve cell death. All thermal ablation interventions are negatively affected by the blood vessel perfusion: nearby macroscopic vessels (larger than 1 mm in diameter) cause the so-called heat/cold sink effect which consists in the dispersion and removal of the heat/cold. This effect will reduce and deform the boundary of the expected coagulation region.

In the case of hepatic interventions, the lung or the costodiaphragmatic recess should be avoided in order to prevent a pneumothorax. Blood vessels should also be avoided: hepatic and superior epigastric vessels should not be crossed in order to prevent bleeding and pain. Bone structures such as the ribs represent an obstacle that prevents to reach the target. Furthermore, nerves beneath the ribs can cause considerable pain and neurological deficits if injured. Fig. 4 shows example trajectories aimed to reach a deep-seated location in the liver.

In terms of the feasibility of the procedure, the chosen path should consider four key factors:

- *the length* of the chosen path should be as short as possible in order to minimize the deviation from the planned path during the intervention;
- *the angle* between the path and the axial plane (vertical angulation) should be as low as possible, in-plane trajectories being easier to perform;
- the in-plane orientation (i.e., left, anterior, right, posterior) of the selected access paths has to conform to the standard local clinical workflow;
- the collision with the scanner should be avoided, and the comfort of the patient and of the interventional radiologist should be promoted.

It has been widely noted that the success of these procedure hinges greatly on its pre-operative planning (Baegert et al. (2007b,c)), which requires the identification of the anatomical

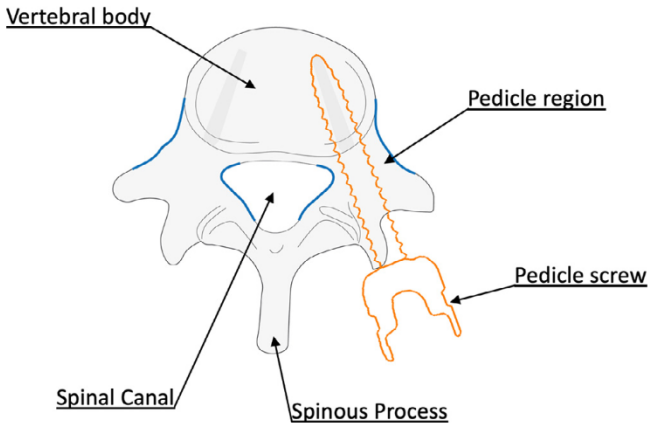

Fig. 5. Example of pedicle screw insertion. The screw is inserted to a previously drilled canal in the pedicle region. The screw must be correctly positioned to avoid the breach of the anterior cortical bone and pedicles boundaries.

structures in the abdominal cavity and the location of the tumor for its histopathological evaluation or for its ablative treatment.

The identification and reconstruction of extra-hepatic structures (including the ribs, celiac artery/vein, spine, lung, stomach, and spleen) and intrahepatic tissues (including the liver, liver vessels, and liver tumor) is of utmost importance for the pre-operative planning of these procedures. Chen et al. (2017) segmented liver, bone, skin and hepatic tumors by a region-appearance-based adaptive variational model proposed in Peng et al. (2014). Thresholding and region growing techniques were used in Helck et al. (2016); Ebert et al. (2016); Schumann et al. (2015). Ren et al. (2014) applied a semi-automatic segmentation method using the ITK-SNAP program's geodesic active contour method (Yushkevich et al. (2006)) to identify the key structures including the tumor and structures that should not be traversed such as the ribs, liver vasculature, and adjacent critical anatomical structures.

4.3. Spinal fusion

Vertebral fixation is a surgical procedure for the treatment of different types of spinal column disorders including neurological deficits or severe pain caused by ruptured or slipped discs, degenerative disc disease, vertebral fracture, stenosis, spondylolisthesis, and spinal disc herniation. The spinal fixation is used for fusing together and/or mechanically immobilizing vertebrae of the spine. One of the most used techniques is the pedicle screw placement. It consists in the insertion of screws from the posterior side, by drilling a canal into the vertebra pedicle (Manbachi et al. (2014)). During the procedure, however, clinically relevant screws that are 4.5–8.0 mm in diameter, should be inserted into the lumbar pedicle of the vertebra, which only has a diameter of about 6–10 mm. Failure in doing so may cause unrecoverable damage to the spinal cord, resulting in serious injury to the patient (Di Silvestre et al. (2007)).

Determining the proper size and orientation of pedicle screws in an operating room environment is challenging. If a mistake is made in selecting an appropriate size and/or orientation of the pedicle screw, the consequences for the patient may be severe and cause great injury. In fact, fracturing the pedicle can damage nerve roots, the dural sac, vascular structures, and pleura, while medial breach of the spinal canal is particularly dangerous and can cause paralysis. Fig. 5 shows a graphical representation of a pedicle screw insertion procedure.

Surgical planning algorithms for pedicle screw insertion are bounded to the specific anatomy of the vertebra, and require the identification and segmentation of the different vertebral segments. Most of the solutions provided fall into automated planning algorithms, taking advantage of the reduced variability in the vertebra anatomy. Some authors working on trajectory planning have also proposed their own pipelines for the segmentation of those structures: Wicker and Tedla (2004); Xiaozhao et al. (2016) applied a thresholding method for the segmentation of a single vertebral spine segment, exploiting the large gap between bone and soft tissue intensity values. Further surface extraction was performed via edge detection technique such as sobel, prewitt filters. Lee et al. (2011a) proposed a method for the identification of the vertebra, of the center point of the spinal canal and the spinal pedicle, based on a three-steps algorithm which included i) a dynamic thresholding, ii) an edge matching step and iii) a connected component analysis to isolate only-spine regions from the rest of the structures. A morphological thinning operator was applied to identify the spinal canal, which allowed for the subsequent identification of pedicles. This methodology has been used in Lee et al. (2011b, 2012). Knez et al. (2018a, 2018b, 2016a, 2015, 2016b) used a parametric modelling based on superquadrics. The 3D vertebral body shape model was represented in the form of an elliptical cylinder, and deformed by introducing additional shape parameters and aligned to the observed vertebral body in the CT image by maximizing the similarity between the 3D model and the corresponding anatomy. A analog procedure was applied to obtain the 3D pedicle models.

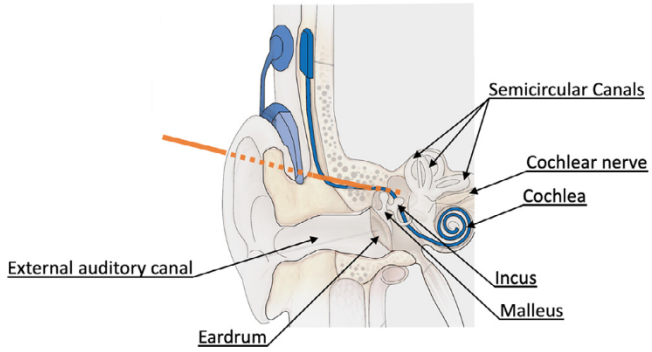

Fig. 6. Example of cochlear implant surgery. The drilled trajectory must reach the entrance of cochlea without damaging the surrounding structures. In the anatomical image are reported some of the most sensitive anatomical structures.

4.4. Maxillo-facial and ENT surgery

Articles focused on Maxillo and ENT surgery constitute a minor part of the results. However, they follow the general principles related to surgical planning modelling. While only Gao et al. (2014) focused on cranio-facial surgery, the remaining articles present methods for lateral skull based interventions (Becker et al. (2013, 2012)), which include cochlea implant surgery (Wimmer et al. (2014); Gerber et al. (2014); Noble et al. (2010a); Al-Marzouqi et al. (2007)). The minimally invasive percutaneous access to the cochlea requires the drilling of a small tunnel from the outer surface of the mastoid, passing through the facial recess and reaching the cochlea without damaging any sensitive surrounding structure as the facial nerve, the external of the auditory canal, the chorda tympani and the ossicles (the malleus, incus and stape). Fig. 6 reports an example of cochlear implant.

From the mastoid surface to the cochlea, all of the above mentioned critical structures are contained within a region which ranges between 1.0 - 3.5 mm in diameter (Noble et al. (2010a)), through which the trajectory must also pass. Previous studies demonstrated that a drilling accuracy of at least 0.5 mm would be sufficient to safely drill through the facial recess without causing any damage to surrounding structures (Schipper et al. (2004)).

Table 5
Combination of words used in the systematic review. The words within each group where searched with an 'OR' connection, while between groups we applied an 'AND' connection.

group 1	group 2	group 3	group 4
Automat(ic, ed) Computeri(s/z)ed Computer - assisted, aided	surgical surgery percutaneous needle(s) screw(s) keyhole biopsy(ies) probe(s)	plan planning	trajectory -ies path(s)

Therefore, the identification and segmentation of those anatomical regions is mandatory for the development of automated surgical planning algorithms.

In Becker et al. (2013, 2012), a simple thresholding method was used for the segmentation of the cranial bone. However, all the internal structures were manually labelled from the analysis of CT images. In Gerber et al. (2014), the authors used semi-automatic methods, manual thresholding and morphological operators. In Wimmer et al. (2014) the ossicles, the cochlea, the vestibulum, and the semicircular canals were segmented using a region growing algorithm, and manual refinement to remove outliers in the bony labyrinth. With the exception of Noble et al. (2010a), which localized the relevant structures using an atlas-based strategy (Dawant et al. (1999); Rohde et al. (2003)) and specific segmentation pipelines (Noble et al. (2008, 2009, 2010b)), all the reported works require the manual intervention of the user.

5. Conclusions

An extended overview of surgical planning assistance methods focused on percutaneous keyhole interventions based on the insertion of needle-shaped tools has been presented. The systematic review included 113 articles, which have been classified and analyzed from different perspectives. To the authors' knowledge, this is the first systematic literature review that covers needle-shaped trajectory planning assistance from a methodological point of view, without focusing on a single clinical application.

The problem has been presented from a general perspective, describing the principal phases guiding the modelling of percutaneous applications: *image processing* (Section 2.1), *formalization* (Section 2.2), *optimization* (Section 2.3) and *experimental design and validation* (Section 2.4). Along the description of each phase, we provided practical examples by including the references to the articles.

Focusing on optimization schemes, the review revealed that the majority of the works represented the surgical planning problem with an aggregative approach, probably because of its intuitiveness in defining the importance of each constraint. Only few works have explored Pareto-based (Seitel et al. (2011); Schumann et al. (2015); Hamzé et al. (2016)) and evolutionary approaches (Lim et al. (2013); Ren et al. (2014)), which are stated to be more efficient in the resolution of non-convex optimization problems. The great number of solutions exploiting exhaustive search methods suggests that CAP applications have no strict optimization requirements, and brute force methods are an efficient approximation. However, we consider that Pareto-based optimization represents an interesting research area for the future, that could provide more effective and efficient solutions.

We classified the validation experiments based on the type of evaluation performed and the data used, providing a brief description and references of the most relevant experiments. In many cases, the authors passed through many different validation steps (e.g. authors[7] of Epinav™, which represent the most advanced platform in terms of validation experiments), indicating how surgical planning modelling consists in a long and iterative process. However, using the validation provided as an indicator of the TRL, only few systems can be considered close to their inclusion in the clinical practice. In Vakharia et al. (2018b, 2019a), the authors demonstrated the enormous variability in the definition of a safe and optimal trajectory, at least in the SEEG domain. The same problem has been reported for other neurosurgical scenarios, which represent almost 50% of the available literature. There are no standard rules to directly compare the quality of the proposed assistance, that is also greatly influenced by the different medical workflows of clinical centers (which include medical image scans, segmentation methods, the hardware used for the interventions and others). Additionally, every group appears to use its own solution regarding the segmentation of relevant structures, preventing a direct comparison between planning algorithms in terms of quantitative analysis.

Different clinical applications have been found from the literature research, presented in Section 4. While each clinical intervention has its own requirements, it can be stated that they share a common base and many of the algorithms could be easily adapted to other domains. Actually, a general framework (similar to the one proposed in Baegert et al. (2007c)) could provide a solution adaptable to many of the interventions reported. Accordingly, in Section 3 we presented many similar algorithms applied to different applications (especially abdominal and neurosurgical procedures).

In our opinion, a fundamental requirement of those systems is their usability: accurate anatomical segmentation seems to be one of the major problems directly bounded to the anatomy of interest and by which the results of a planning assistant are deeply influenced. While neurosurgical and abdominal applications can take advantage of a wide literature on segmentation algorithms, spine, maxillo and ENT applications may require to implement their own solutions. Especially the latter, which requires the precise segmentation of small anatomical parts, did not present a robust segmentation pipeline and manual intervention was often required, which may prevent those systems to be widely used in the near future.

Finally, all the articles reported in this work assume perfectly straight needle trajectories, with no deformation occurring during the insertion. This specific problem has been addressed only in Hamzé et al. (2015) and would certainly deserve more attention.

Appendix - Systematic search

We searched for publications on the topic of automatic planning in surgery on PubMed, Scopus, ISI Web of Science, in date 24/10/2019. The research included all the different combination of 4 groups of words, reported in Table 5.

The choice of such strict queries was determined by the specific topic covered by the review. To guarantee that all the relevant works were considered, we reviewed the bibliography of each paper contained in the study for additional citations.

Inclusion/Exclusion Criteria

In the review, we included all the papers that described a software application able to assist the surgeons during the planning phase of percutaneous surgeries. Automated, semi-automated or interactive approaches aiming to simplify the trajectory definition

[7] Zombori et al. (2014); Sparks et al. (2017a,b); Nowell et al. (2016); Vakharia et al. (2018a, 2018b, 2019a, 2019b); Li et al. (2019a)

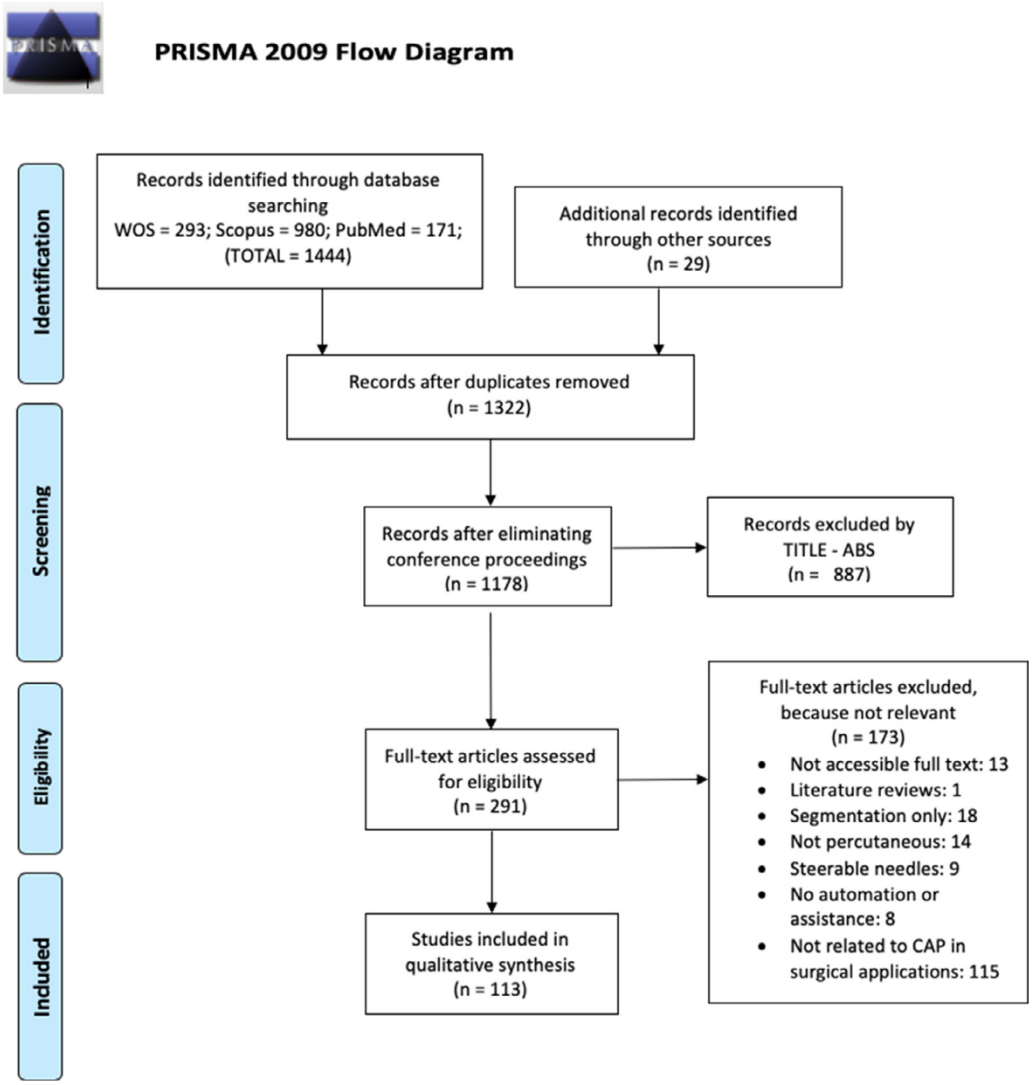

Fig. 7. PRISMA (Preferred Reporting Items for Systematic Reviews and Meta-Analyses) diagram for the systematic identification, screening and included articles in the review.

have been considered. We intended as assistance all software solutions able to provide a quantitative feedback regarding the safety and effectiveness of the trajectory, or methods aimed to optimize specific parameters of the surgery based on clinical considerations. The search was limited to the last 19 years (from 2000) and only papers written in English were taken into account. We voluntarily discarded all the articles focused on steerable needles or describing the modeling approaches about needle-soft tissue interaction. We considered those works to be related on the implementation of new prototypes for robotic surgery, or to provide a realistic simulation between tissues and needles. The aim of this survey was to revise the actual state of art in modeling and automatization of the preoperative planning phase based on the clinical requirements of percutaneous procedures.

The results of the literature search are presented in Fig. 7, represented in a workflow diagram as proposed by the PRISMA statement (Moher et al. (2009)).

Declaration of Competing Interest

The authors declare that they have no known competing financial interests or personal relationships that could have appeared to influence the work reported in this paper.

CRediT authorship contribution statement

Davide Scorza: Conceptualization, Data curation, Formal analysis, Writing - original draft, Writing - review & editing. **Sara El Hadji:** Formal analysis, Data curation, Writing - original draft. **Camilo Cortés:** Writing - review & editing, Formal analysis, Supervision. **Álvaro Bertelsen:** Project administration, Funding acquisition. **Francesco Cardinale:** Supervision, Formal analysis. **Giuseppe Baselli:** Supervision. **Caroline Essert:** Writing - review & editing, Formal analysis, Supervision. **Elena De Momi:** Supervision, Formal analysis.

Acknowledgment

This research is a part of the SINAPSIS Project funded by ELKARTEK 2017 by the industry department of the Basque Country.

References

Abolhassani, N., Patel, R., Moallem, M., 2007. Needle insertion into soft tissue: a survey. Medical engineering & physics 29 (4), 413–431.

Ahmadi, S.-A., Klein, T., Navab, N., Roth, R., Shamir, R.R., Joskowicz, L., DeMomi, E., Ferrigno, G., Antiga, L., Foroni, R.I., 2009. Advanced planning and intra-operative validation for robot-assisted keyhole neurosurgery in ROBOCAST. In: 2009 International Conference on Advanced Robotics. IEEE, pp. 1–7.

Al-Marzouqi, H., Noble, J.H., Warren, F.M., Labadie, R.F., Fitzpatrick, J.M., Dawant, B., 2007. Planning a safe drilling path for cochlear implantation surgery using image registration techniques. In: Medical Imaging 2007: Visualization and Image-Guided Procedures, 6509. International Society for Optics and Photonics, p. 650933.

Altrogge, I., Kröger, T., Preusser, T., Büskens, C., Pereira, P.L., Schmidt, D., Weihusen, A., Peitgen, H.-O., 2006. Towards optimization of probe placement for radio-frequency ablation. In: International Conference on Medical Image Computing and Computer-Assisted Intervention. Springer, pp. 486–493.

Altrogge, I., Preusser, T., Kröger, T., Büskens, C., Pereira, P.L., Schmidt, D., Peitgen, H.-O., 2007. Multiscale optimization of the probe placement for radiofrequency ablation. Acad. Radiol. 14 (11), 1310–1324.

Andersson, J., 2000. A survey of multiobjective optimization in engineering design. Department of Mechanical Engineering, Linktjping University. Sweden.

Baegert, C., Villard, C., Schreck, P., Soler, L., 2007. Multi-criteria trajectory planning for hepatic radiofrequency ablation. In: International Conference on Medical Image Computing and Computer-Assisted Intervention. Springer, pp. 676–684.

Baegert, C., Villard, C., Schreck, P., Soler, L., 2007. Precise determination of regions of interest for hepatic RFA planning. In: Medical Imaging 2007: Visualization and Image-Guided Procedures, 6509. International Society for Optics and Photonics, p. 650923.

Baegert, C., Villard, C., Schreck, P., Soler, L., Gangi, A., 2007. Trajectory optimization for the planning of percutaneous radiofrequency ablation of hepatic tumors. Computer Aided Surgery 12 (2), 82–90.

Baissalov, R., Sandison, G.A., Reynolds, D., Muldrew, K., 2001. Simultaneous optimization of cryoprobe placement and thermal protocol for cryosurgery. Physics in Medicine & Biology 46 (7), 1799.

Bakhshmand, S.M., Eagleson, R., de Ribaupierre, S., 2017. Multimodal connectivity based eloquence score computation and visualisation for computer-aided neurosurgical path planning 4, 152–156. doi:10.1049/htl.2017.0073.

Becker, M., Gutbell, R., Stenin, I., Wesarg, S., 2012. Towards automatic path planning for multi-port minimally-traumatic lateral skull base surgery. In: Workshop on Clinical Image-Based Procedures. Springer, pp. 59–66.

Becker, M., Hansen, S., Wesarg, S., Sakas, G., 2013. Path planning for multi-port lateral skull base surgery based on first clinical experiences. In: Workshop on Clinical Image-Based Procedures. Springer, pp. 23–30.

Belbachir, E., Golkar, E., Bayle, B., Essert, C., 2018. Automatic planning of needle placement for robot-assisted percutaneous procedures. Int. J. Comput. Assist. Radiol. Surg. 13 (9), 1429–1438.

Benabid, A.L., Chabardes, S., Mitrofanis, J., Pollak, P., 2009. Deep brain stimulation of the subthalamic nucleus for the treatment of parkinson's disease. The Lancet Neurology 8 (1), 67–81.

Berber, E., 2015. The first clinical application of planning software for laparoscopic microwave thermosphere ablation of malignant liver tumours. HPB 17 (7), 632–636.

Bériault, S., Al Subaie, F., Collins, D.L., Sadikot, A.F., Pike, G.B., 2012. A multi-modal approach to computer-assisted deep brain stimulation trajectory planning. Int. J. Comput. Assist. Radiol. Surg. 7 (5), 687–704.

Bériault, S., Al Subaie, F., Mok, K., Sadikot, A.F., Pike, G.B., 2011. Automatic trajectory planning of DBS neurosurgery from multi-modal mri datasets. In: International Conference on Medical Image Computing and Computer-Assisted Intervention. Springer, pp. 259–266.

Bériault, S., Drouin, S., Sadikot, A.F., Xiao, Y., Collins, D.L., Pike, G.B., 2012. A prospective evaluation of computer-assisted deep brain stimulation trajectory planning. In: Workshop on Clinical Image-Based Procedures. Springer, pp. 42–49.

Brunenberg, E.J., Vilanova, A., Visser-Vandewalle, V., Temel, Y., Ackermans, L., Platel, B., ter Haar Romeny, B.M., 2007. Automatic trajectory planning for deep brain stimulation: a feasibility study. In: International Conference on Medical Image Computing and Computer-Assisted Intervention. Springer, pp. 584–592.

Butz, T., Warfield, S.K., Tuncali, K., Silverman, S.G., van Sonnenberg, E., Jolesz, F.A., Kikinis, R., 2000. Pre-and intra-operative planning and simulation of percutaneous tumor ablation. In: International Conference on Medical Image Computing and Computer-Assisted Intervention. Springer, pp. 317–326.

Cardoso, M.J., Modat, M., Wolz, R., Melbourne, A., Cash, D., Rueckert, D., Ourselin, S., 2015. Geodesic information flows: spatially-variant graphs and their application to segmentation and fusion. IEEE Trans. Med. Imaging 34 (9), 1976–1988.

Chen, C.-C.R., Miga, M.I., Galloway, R.L., 2006. Optimizing needle placement in treatment planning of radiofrequency ablation. In: Medical Imaging 2006: Visualization, Image-Guided Procedures, and Display, 6141. International Society for Optics and Photonics, p. 614124.

Chen, R., Lu, F., Wang, K., Kong, D., et al., 2017. Semiautomatic radiofrequency ablation planning based on constrained clustering process for hepatic tumors. IEEE Trans. Biomed. Eng. 65 (3), 645–657.

Collins, D.L., Holmes, C.J., Peters, T.M., Evans, A.C., 1995. Automatic 3d model-based neuroanatomical segmentation. Hum. Brain Mapp. 3 (3), 190–208.

Collins, D.L., Neelin, P., Peters, T.M., Evans, A.C., 1994. Automatic 3d inter-subject registration of MR volumetric data in standardized talairach space.. J. Comput. Assist. Tomogr. 18 (2), 192–205.

Collins, D.L., Zijdenbos, A.P., Baaré, W.F., Evans, A.C., 1999. ANIMAL+ INSECT: improved cortical structure segmentation. In: Biennial International Conference on Information Processing in Medical Imaging. Springer, pp. 210–223.

Cui, Y., Geng, Z., Zhu, Q., Han, Y., 2017. Multi-objective optimization methods and application in energy saving. Energy 125, 681–704.

Daemi, N., Ahmadian, A., Mirbagheri, A., Ahmadian, A., Saberi, H., Amidi, F., Alirezaie, J., 2015. Planning screw insertion trajectory in lumbar spinal fusion using pre-operative CT images. In: 2015 37th Annual International Conference of the IEEE Engineering in Medicine and Biology Society (EMBC). IEEE, pp. 3639–3642.

D'Albis, T., Haegelen, C., Essert, C., Fernández-Vidal, S., Lalys, F., Jannin, P., 2015. PyDBS: an automated image processing workflow for deep brain stimulation surgery. Int. J. Comput. Assist. Radiol. Surg. 10 (2), 117–128.

Danielsson, P.-E., 1980. Euclidean distance mapping. Computer Graphics and image processing 14 (3), 227–248.

Dawant, B.M., Hartmann, S.L., Thirion, J.-P., Maes, F., Vandermeulen, D., Demaerel, P., 1999. Automatic 3d segmentation of internal structures of the head in MR images using a combination of similarity and free-form transformations. i. methodology and validation on normal subjects. IEEE Trans. Med. Imaging 18 (10), 909–916.

De León-Cuevas, A., Tovar-Arriaga, S., González-Gutiérrez, A., Aceves-Fernández, M.A., 2017. Risk map generation for keyhole neurosurgery using fuzzy logic for trajectory evaluation. Neurocomputing 233, 81–89.

De Momi, E., Caborni, C., Cardinale, F., Casaceli, G., Castana, L., Cossu, M., Mai, R., Gozzo, F., Francione, S., Tassi, L., et al., 2014. Multi-trajectories automatic planner for stereoelectroencephalography (SEEG). Int. J. Comput. Assist. Radiol. Surg. 9 (6), 1087–1097.

De Momi, E., Caborni, C., Cardinale, F., Castana, L., Casaceli, G., Cossu, M., Antiga, L., Ferrigno, G., 2012. Automatic trajectory planner for stereoelectroencephalography procedures: a retrospective study. IEEE Trans. Biomed. Eng. 60 (4), 986–993.

Deng, Z.-S., Liu, J., 2007. Computerized planning of multi-probe cryosurgical treatment for tumor with complex geometry. In: ASME 2007 International Mechanical Engineering Congress and Exposition. American Society of Mechanical Engineers, pp. 97–101.

Dergachyova, O., Zhao, Y., Haegelen, C., Jannin, P., Essert, C., 2018. Automatic preoperative planning of DBS electrode placement using anatomo-clinical atlases and volume of tissue activated. Int. J. Comput. Assist. Radiol. Surg. 13 (7), 1117–1128.

D'Haese, P.-F., Cetinkaya, E., Konrad, P.E., Kao, C., Dawant, B.M., 2005. Computer-aided placement of deep brain stimulators: from planning to intraoperative guidance. IEEE Trans. Med. Imaging 24 (11), 1469–1478.

D'Haese, P.-F., Pallavaram, S., Li, R., Remple, M.S., Kao, C., Neimat, J.S., Konrad, P.E., Dawant, B.M., 2012. Cranialvault and its crave tools: a clinical computer assistance system for deep brain stimulation (DBS) therapy. Med. Image Anal. 16 (3), 744–753.

Di Silvestre, M., Parisini, P., Lolli, F., Bakaloudis, G., 2007. Complications of thoracic pedicle screws in scoliosis treatment. Spine 32 (15), 1655–1661.

Dodd, G.D., Frank, M.S., Aribandi, M., Chopra, S., Chintapalli, K.N., 2001. Radiofrequency thermal ablation: computer analysis of the size of the thermal injury created by overlapping ablations. American Journal of Roentgenology 177 (4), 777–782.

Ebert, L.C., Fürst, M., Ptacek, W., Ruder, T.D., Gascho, D., Schweitzer, W., Thali, M.J., Flach, P.M., 2016. Automatic entry point planning for robotic post-mortem CT-based needle placement. Forensic Sci. Med. Pathol. 12 (3), 336–342.

Essert, C., Fernandez-Vidal, S., Capobianco, A., Haegelen, C., Karachi, C., Bardinet, E., Marchal, M., Jannin, P., 2015. Statistical study of parameters for deep brain stimulation automatic preoperative planning of electrodes trajectories. Int. J. Comput. Assist. Radiol. Surg. 10 (12), 1973–1983.

Essert, C., Haegelen, C., Jannin, P., 2010. Automatic computation of electrodes trajectory for deep brain stimulation. In: International Workshop on Medical Imaging and Virtual Reality. Springer, pp. 149–158.

Essert, C., Haegelen, C., Lalys, F., Abadie, A., Jannin, P., 2012. Automatic computation of electrode trajectories for deep brain stimulation: a hybrid symbolic and numerical approach. Int. J. Comput. Assist. Radiol. Surg. 7 (4), 517–532.

Essert, C., Marchal, M., Fernandez-Vidal, S., D'Albis, T., Bardinet, E., Haegelen, C., Welter, M.-L., Yelnik, J., Jannin, P., 2012. Automatic parameters optimization for deep brain stimulation trajectory planning. In: Proceedings of MICCAI workshop DBSMC, 12, pp. 20–29.

Essert, C., Rao, P.P., Gangi, A., Joskowicz, L., 2019. 3D modelling of the residual freezing for renal cryoablation simulation and prediction. In: International Conference on Medical Image Computing and Computer-Assisted Intervention. Springer, pp. 209–217.

Favaro, A., Lad, A., Formenti, D., Zani, D.D., De Momi, E., 2017. Straight trajectory planning for keyhole neurosurgery in sheep with automatic brain structures segmentation. In: Medical Imaging 2017: Image-Guided Procedures, Robotic Interventions, and Modeling, 10135. International Society for Optics and Photonics, p. 101352E.

Fischl, B., 2012. Freesurfer. Neuroimage 62 (2), 774–781.

Fischl, B., Salat, D.H., Busa, E., Albert, M., Dieterich, M., Haselgrove, C., Van Der Kouwe, A., Killiany, R., Kennedy, D., Klaveness, S., et al., 2002. Whole brain segmentation: automated labeling of neuroanatomical structures in the human brain. Neuron 33 (3), 341–355.

Frangi, A.F., Niessen, W.J., Vincken, K.L., Viergever, M.A., 1998. Multiscale vessel enhancement filtering. In: International conference on medical image computing and computer-assisted intervention. Springer, pp. 130–137.

Freiman, M., Joskowicz, L., Broide, N., Natanzon, M., Nammer, E., Shilon, O., Weizman, L., Sosna, J., 2012. Carotid vasculature modeling from patient CT angiography studies for interventional procedures simulation. Int. J. Comput. Assist. Radiol. Surg. 7 (5), 799–812.

Gao, C., Chen, L., Hou, B., Liu, X., Guo, C., 2014. Precise and semi-automatic puncture trajectory planning in craniofacial surgery: A prototype study. In: 2014 7th International Conference on Biomedical Engineering and Informatics. IEEE, pp. 617–622.

Gerber, N., Bell, B., Gavaghan, K., Weisstanner, C., Caversaccio, M., Weber, S., 2014. Surgical planning tool for robotically assisted hearing aid implantation. Int. J. Comput. Assist. Radiol. Surg. 9 (1), 11–20.
Goerres, J., Uneri, A., De Silva, T., Ketcha, M., Reaungamornrat, S., Jacobson, M., Vogt, S., Kleinszig, G., Osgood, G., Wolinsky, J., et al., 2017. Spinal pedicle screw planning using deformable atlas registration. Physics in Medicine & Biology 62 (7), 2871.
Goerres, J., Uneri, A., Jacobson, M., Ramsay, B., De Silva, T., Ketcha, M., Han, R., Manbachi, A., Vogt, S., Kleinszig, G., et al., 2017. Planning, guidance, and quality assurance of pelvic screw placement using deformable image registration. Physics in Medicine & Biology 62 (23), 9018.
Golkar, E., Rao, P.P., Joskowicz, L., Gangi, A., Essert, C., 2018. Fast gpu computation of 3D isothermal volumes in the vicinity of major blood vessels for multiprobe cryoablation simulation. In: International Conference on Medical Image Computing and Computer-Assisted Intervention. Springer, pp. 230–237.
Gravante, G., Ong, S.L., Metcalfe, M.S., Strickland, A., Dennison, A.R., Lloyd, D.M., 2008. Hepatic microwave ablation: a review of the histological changes following thermal damage. Liver international 28 (7), 911–921.
Greene, N., 1986. Environment mapping and other applications of world projections. IEEE Comput. Graph. Appl. 6 (11), 21–29.
Guo, T., Parrent, A.G., Peters, T.M., 2007. Automatic target and trajectory identification for deep brain stimulation (DBS) procedures. In: International Conference on Medical Image Computing and Computer-Assisted Intervention. Springer, pp. 483–490.
Hamzé, N., Bilger, A., Duriez, C., Cotin, S., Essert, C., 2015. Anticipation of brain shift in deep brain stimulation automatic planning. In: 2015 37th Annual International Conference of the IEEE Engineering in Medicine and Biology Society (EMBC). IEEE, pp. 3635–3638.
Hamzé, N., Voirin, J., Collet, P., Jannin, P., Haegelen, C., Essert, C., 2016. Pareto front vs. weighted sum for automatic trajectory planning of deep brain stimulation. In: International Conference on Medical Image Computing and Computer-Assisted Intervention. Springer, pp. 534–541.
Han, R., Uneri, A., De Silva, T., Ketcha, M., Goerres, J., Vogt, S., Kleinszig, G., Osgood, G., Siewerdsen, J., 2019. Atlas-based automatic planning and 3d-2dfluoroscopic guidance in pelvic trauma surgery. Physics in Medicine & Biology 64 (9), 095022.
Héder, M., 2017. From NASA to EU: the evolution of the TRL scale in public sector innovation. The Innovation Journal 22 (2), 1–23.
Helck, A., Schumann, C., Aumann, J., Thierfelder, K., Strobl, F., Braunagel, M., Niethammer, M., Clevert, D.-A., Hoffmann, R.-T., Reiser, M., et al., 2016. Automatic path proposal computation for CT-guided percutaneous liver biopsy. Int. J. Comput. Assist. Radiol. Surg. 11 (12), 2199–2205.
Herghelegiu, P., Manta, V., Gröller, E., 2011. Needle-stability maps for brain-tumor biopsies. In: 15th International Conference on System Theory, Control and Computing. IEEE, pp. 1–5.
Herghelegiu, P.-C., Manta, V., Perin, R., Bruckner, S., Gröller, E., 2012. Biopsy planner-visual analysis for needle pathway planning in deep seated brain tumor biopsy. In: Computer graphics forum, 31. Wiley Online Library, pp. 1085–1094.
Herzog, J., Fietzek, U., Hamel, W., Morsnowski, A., Steigerwald, F., Schrader, B., Weinert, D., Pfister, G., Müller, D., Mehdorn, H.M., et al., 2004. Most effective stimulation site in subthalamic deep brain stimulation for parkinson's disease. Movement disorders 19 (9), 1050–1054.
Huang, S., Yu, J., Liang, P., Yu, X., Cheng, Z., Han, Z., Li, Q., 2014. Percutaneous microwave ablation for hepatocellular carcinoma adjacent to large vessels: a long-term follow-up. Eur. J. Radiol. 83 (3), 552–558.
Jaberzadeh, A., Essert, C., 2016. Pre-operative planning of multiple probes in three dimensions for liver cryosurgery: comparison of different optimization methods. Math. Methods Appl. Sci. 39 (16), 4764–4772.
Jiang, S., Liu, X., Song, Y., 2009. 3D trajectory planning based on FEM with application of brachytherapy. In: 2009 2nd International Conference on Biomedical Engineering and Informatics. IEEE, pp. 1–5.
Kang, X., Ren, H., Li, J., Yau, W.-P., 2012. Statistical atlas based registration and planning for ablating bone tumors in minimally invasive interventions. In: 2012 IEEE International Conference on Robotics and Biomimetics (ROBIO). IEEE, pp. 606–611.
Karras, T., 2012. Maximizing parallelism in the construion of BVHs, orees, and k-d trees. In: Proceedings of the Fourth ACM SIGGRAPH/Eurographics conference on High-Performance Graphics. Eurographics Association, pp. 33–37.
Khlebnikov, R., Kainz, B., Muehl, J., Schmalstieg, D., 2011. Crepuscular rays for tumor accessibility planning. IEEE Trans. Vis. Comput. Graph. 17 (12), 2163–2172.
Kirkpatrick, S., Gelatt, C.D., Vecchi, M.P., 1983. Optimization by simulated annealing. Science 220 (4598), 671–680.
Klein, A., Tourville, J., 2012. 101 Labeled brain images and a consistent human cortical labeling protocol. Front. Neurosci. 6, 171.
Klein, S., Whyne, C.M., Rush, R., Ginsberg, H.J., 2009. Ct-based patient-specific simulation software for pedicle screw insertion. Clinical Spine Surgery 22 (7), 502–506.
Knez, D., Likar, B., Pernuš, F., Vrtovec, T., 2015. Automated pedicle screw size and trajectory planning by maximization of fastening strength. In: International Workshop and Challenge on Computational Methods and Clinical Applications for Spine Imaging. Springer, pp. 3–13.
Knez, D., Likar, B., Pernuš, F., Vrtovec, T., 2016. Computer-assisted screw size and insertion trajectory planning for pedicle screw placement surgery. IEEE Trans. Med. Imaging 35 (6), 1420–1430.
Knez, D., Mohar, J., Cirman, R.J., Likar, B., Pernuš, F., Vrtovec, T., 2016. Manual and computer-assisted pedicle screw placement plans: a quantitative comparison. In: International Workshop on Computational Methods and Clinical Applications for Spine Imaging. Springer, pp. 105–115.
Knez, D., Mohar, J., Cirman, R.J., Likar, B., Pernuš, F., Vrtovec, T., 2018. Variability analysis of manual and computer-assisted preoperative thoracic pedicle screw placement planning. Spine 43 (21), 1487–1495.
Knez, D., Nahle, I.S., Vrtovec, T., Parent, S., Kadoury, S., 2018. Computer-assisted pedicle screw placement planning: Towards clinical practice. In: 2018 IEEE 15th International Symposium on Biomedical Imaging (ISBI 2018). IEEE, pp. 249–252.
Knez, D., Nahle, I.S., Vrtovec, T., Parent, S., Kadoury, S., 2019. Computer-assisted pedicle screw trajectory planning using CT-inferred bone density: a demonstration against surgical outcomes. Med. Phys..
Krag, M.H., Beynnon, B.D., Pope, M.H., DeCoster, T.A., 1988. Depth of insertion of transpedicular vertebral screws into human vertebrae: effect upon screw-vertebra interface strength.. J. Spinal. Disord. 1 (4), 287–294.
Le Goualher, G., Barillot, C., Bizais, Y., 1997. Modeling cortical sulci with active ribbons. Int. J. Pattern Recognit Artif Intell. 11 (08), 1295–1315.
Lee, J., Kim, S., Kim, Y.S., Chung, W.K., 2011. Automated segmentation of the lumbar pedicle in CT images for spinal fusion surgery. IEEE Trans. Biomed. Eng. 58 (7), 2051–2063.
Lee, J., Kim, S., Kim, Y.S., Chung, W.K., 2012. Optimal surgical planning guidance for lumbar spinal fusion considering operational safety and vertebra–screw interface strength. The International Journal of Medical Robotics and Computer Assisted Surgery 8 (3), 261–272.
Lee, J., Kim, S., Kim, Y.S., Chung, W.K., Kim, M., 2011. Automated surgical planning and evaluation algorithm for spinal fusion surgery with three-dimensional pedicle model. In: 2011 IEEE/RSJ International Conference on Intelligent Robots and Systems. IEEE, pp. 2524–2531.
Lehman Jr, R.A., Polly Jr, D.W., Kuklo, T.R., Cunningham, B., Kirk, K.L., Belmont Jr, P.J., 2003. Straight-forward versus anatomic trajectory technique of thoracic pedicle screw fixation: a biomechanical analysis. Spine 28 (18), 2058–2065.
Li, K., Vakharia, V.N., Sparks, R., França, L.G., Granados, A., McEvoy, A.W., Miserocchi, A., Wang, M., Ourselin, S., Duncan, J.S., 2019. Optimizing trajectories for cranial laser interstitial thermal therapy using computer-assisted planning: a machine learning approach. Neurotherapeutics 16 (1), 182–191.
Li, K., Vakharia, V.N., Sparks, R., Rodionov, R., Vos, S.B., McEvoy, A.W., Miserocchi, A., Wang, M., Ourselin, S., Duncan, J.S., 2019. Stereoelectroencephalography electrode placement: detection of blood vessel conflicts. Epilepsia 60 (9), 1942–1948.
Lim, W.C., Guo, W., Ren, H., 2013. An ablation planning system for computer-assisted interventions. In: 2013 International Conference on Collaboration Technologies and Systems (CTS). IEEE, pp. 487–490.
Linte, C.A., Camp, J.J., Augustine, K.E., Huddleston, P.M., Robb, R.A., Holmes III, D.R., 2015. Estimating pedicle screw fastening strength via a virtual templating platform for spine surgery planning: a retrospective preliminary clinical demonstration. Computer Methods in Biomechanics and Biomedical Engineering: Imaging & Visualization 3 (4), 204–212.
Liu, S., Xia, Z., Liu, J., Xu, J., Ren, H., Lu, T., Yang, X., 2016. Automatic multiple-needle surgical planning of robotic-assisted microwave coagulation in large liver tumor therapy. PLoS ONE 11 (3), e0149482.
Liu, Y., Dawant, B.M., Pallavaram, S., Neimat, J.S., Konrad, P.E., D'Haese, P.-F., Datteri, R.D., Landman, B.A., Noble, J.H., 2012. A surgeon specific automatic path planning algorithm for deep brain stimulation. In: Medical Imaging 2012: Image-Guided Procedures, Robotic Interventions, and Modeling, 8316. International Society for Optics and Photonics, p. 83161D.
Liu, Y., Konrad, P.E., Neimat, J.S., Tatter, S.B., Yu, H., Datteri, R.D., Landman, B.A., Noble, J.H., Pallavaram, S., Dawant, B.M., et al., 2014. Multisurgeon, multisite validation of a trajectory planning algorithm for deep brain stimulation procedures. IEEE Trans. Biomed. Eng. 61 (9), 2479–2487.
Lorensen, W.E., Cline, H.E., 1987. Marching cubes: A high resolution 3D surface construion algorithm. In: ACM siggraph computer graphics, 21. ACM, pp. 163–169.
Lung, D.C., Stahovich, T.F., Rabin, Y., 2004. Computerized planning for multiprobe cryosurgery using a force-field analogy. Comput. Methods Biomech. Biomed. Engin. 7 (2), 101–110.
Mack, M.J., 2001. Minimally invasive and robotic surgery. JAMA 285 (5), 568–572.
Maks, C.B., Butson, C.R., Walter, B.L., Vitek, J.L., McIntyre, C.C., 2009. Deep brain stimulation activation volumes and their association with neurophysiological mapping and therapeutic outcomes. Journal of Neurology, Neurosurgery & Psychiatry 80 (6), 659–666.
Manbachi, A., Cobbold, R.S., Ginsberg, H.J., 2014. Guided pedicle screw insertion: techniques and training. The Spine Journal 14 (1), 165–179.
Mangin, J.-F., Riviere, D., Cachia, A., Duchesnay, E., Cointepas, Y., Papadopoulos-Orfanos, D., Scifo, P., Ochiai, T., Brunelle, F., Regis, J., 2004. A framework to study the cortical folding patterns. Neuroimage 23, S129–S138.
Mankins, J.C., 1995. Technology readiness levels. White Paper, April 6, 1995.
Marcus, H.J., Vakharia, V.N., Sparks, R., Rodionov, R., Kitchen, N., McEvoy, A.W., Miserocchi, A., Thorne, L., Ourselin, S., Duncan, J.S., 2019. Computer-assisted versus manual planning for stereotactic brain biopsy: a retrospective comparative pilot study. Operative Neurosurgery.
Marler, R.T., Arora, J.S., 2004. Survey of multi-objeive optimization methods for engineering. Struct. Multidiscip. Optim. 26 (6), 369–395.
Marszalik, D., Rączka, W., 2019. Surgical tool trajectory optimization in brain tumour resection. In: 2019 20th International Carpathian Control Conference (ICCC). IEEE, pp. 1–4.
Martin, R.C., Scoggins, C.R., McMasters, K.M., 2010. Safety and efficacy of microwave ablation of hepatic tumors: a prospective review of a 5-year experience. Ann. Surg. Oncol. 17 (1), 171–178.

Mendel, T., Radetzki, F., Wohlrab, D., Stock, K., Hofmann, G.O., Noser, H., 2013. Ct-based 3d visualisation of secure bone corridors and optimal trajectories for sacroiliac screws. Injury 44 (7), 957–963.
Mikos, A., Bowers, D., Noecker, A., McIntyre, C., Won, M., Chaturvedi, A., Foote, K., Okun, M., 2011. Patient-specific analysis of the relationship between the volume of tissue activated during DBS and verbal fluency. Neuroimage 54, S238–S246.
Moccia, S., De Momi, E., El Hadji, S., Mattos, L.S., 2018. Blood vessel segmentation algorithms review of methods, datasets and evaluation metrics. Comput. Methods Programs Biomed. 158, 71–91.
Moher, D., Liberati, A., Tetzlaff, J., Altman, D.G., 2009. Preferred reporting items for systematic reviews and meta-analyses: the PRISMA statement. Ann. Intern. Med. 151 (4), 264–269.
Mullin, J.P., Shriver, M., Alomar, S., Najm, I., Bulacio, J., Chauvel, P., Gonzalez–Martinez, J., 2016. Is SEEG safe? a systematic review and meta-analysis of stereo-electroencephalography–related complications. Epilepsia 57 (3), 386–401.
Navkar, N.V., Tsekos, N.V., Stafford, J.R., Weinberg, J.S., Deng, Z., 2010. Visualization and planning of neurosurgical interventions with straight access. In: International Conference on Information Processing in Computer-Assisted Interventions. Springer, pp. 1–11.
Nelder, J.A., Mead, R., 1965. A simplex method for function minimization. Comput. J. 7 (4), 308–313.
Noble, J.H., Dawant, B.M., Warren, F.M., Labadie, R.F., 2009. Automatic identification and 3d rendering of temporal bone anatomy. Otology & neurotology: official publication of the American Otological Society, American Neurotology Society [and] European Academy of Otology and Neurotology 30 (4), 436.
Noble, J.H., Majdani, O., Labadie, R.F., Dawant, B., Fitzpatrick, J.M., 2010. Automatic determination of optimal linear drilling trajectories for cochlear access accounting for drill-positioning error. The International Journal of Medical Robotics and Computer Assisted Surgery 6 (3), 281–290.
Noble, J.H., Rutherford, R.B., Labadie, R.F., Majdani, O., Dawant, B.M., 2010. Modeling and segmentation of intra-cochlear anatomy in conventional CT. In: Medical Imaging 2010: Image Processing, 7623. International Society for Optics and Photonics, p. 762302.
Noble, J.H., Warren, F.M., Labadie, R.F., Dawant, B.M., 2008. Automatic segmentation of the facial nerve and chorda tympani in CT images using spatially dependent feature values. Med. Phys. 35 (12), 5375–5384.
Nowell, M., Sparks, R., Zombori, G., Miserocchi, A., Rodionov, R., Diehl, B., Wehner, T., Baio, G., Trevisi, G., Tisdall, M., et al., 2016. Comparison of computer-assisted planning and manual planning for depth electrode implantations in epilepsy. J. Neurosurg. 124 (6), 1820–1828.
Nowinski, W.L., Yang, G.L., Yeo, T.T., 2000. Computer-aided stereotactic functional neurosurgery enhanced by the use of the multiple brain atlas database. IEEE Trans. Med. Imaging 19 (1), 62–69.
Ochsner, J.L., 2000. Minimally invasive surgical procedures. Ochsner J. 2 (3), 135–136.
Peng, J., Dong, F., Chen, Y., Kong, D., 2014. A region-appearance-based adaptive variational model for 3d liver segmentation. Med. Phys. 41 (4), 043502.
Pennes, H.H., 1948. Analysis of tissue and arterial blood temperatures in the resting human forearm. J. Appl. Physiol. 1 (2), 93–122.
Powell, M.J., 1964. An efficient method for finding the minimum of a function of several variables without calculating derivatives. Comput. J. 7 (2), 155–162.
Ren, H., Campos-Nanez, E., Yaniv, Z., Banovac, F., Abeledo, H., Hata, N., Cleary, K., 2013. Treatment planning and image guidance for radiofrequency ablation of large tumors. IEEE J. Biomed. Health Inform. 18 (3), 920–928.
Ren, H., Guo, W., Ge, S.S., Lim, W., 2014. Coverage planning in computer-assisted ablation based on genetic algorithm. Comput. Biol. Med. 49, 36–45.
Rincón-Nigro, M., Navkar, N.V., Tsekos, N.V., Deng, Z., 2013. GPU-Accelerated interactive visualization and planning of neurosurgical interventions. IEEE Comput. Graph. Appl. 34 (1), 22–31.
Rivière, D., Geffroy, D., Denghien, I., Souedet, N., Cointepas, Y., 2009. BrainVISA: an extensible software environment for sharing multimodal neuroimaging data and processing tools. Neuroimage 47.
Rohde, G.K., Aldroubi, A., Dawant, B.M., 2003. The adaptive bases algorithm for intensity-based nonrigid image registration. IEEE Trans. Med. Imaging 22 (11), 1470–1479.
Saaty, T.L., 2008. Decision making with the analytic hierarchy process. International journal of services sciences 1 (1), 83–98.
Saint-Cyr, J.A., Hoque, T., Pereira, L.C., Dostrovsky, J.O., Hutchison, W.D., Mikulis, D.J., Abosch, A., Sime, E., Lang, A.E., Lozano, A.M., 2002. Localization of clinically effective stimulating electrodes in the human subthalamic nucleus on magnetic resonance imaging. J. Neurosurg. 97 (5), 1152–1166.
Schipper, J., Aschendorff, A., Arapakis, I., Klenzner, T., Teszler, C.B., Ridder, G.J., Laszig, R., 2004. Navigation as a quality management tool in cochlear implant surgery. The Journal of Laryngology & Otology 118 (10), 764–770.
Schumann, C., Bieberstein, J., Braunewell, S., Niethammer, M., Peitgen, H.-O., 2012. Visualization support for the planning of hepatic needle placement. Int. J. Comput. Assist. Radiol. Surg. 7 (2), 191–197.
Schumann, C., Bieberstein, J., Trumm, C., Schmidt, D., Bruners, P., Niethammer, M., Hoffmann, R.T., Mahnken, A.H., Pereira, P.L., Peitgen, H.-O., 2010. Fast automatic path proposal computation for hepatic needle placement. In: Medical Imaging 2010: Visualization, Image-Guided Procedures, and Modeling, 7625. International Society for Optics and Photonics, p. 76251J.
Schumann, C., Rieder, C., Bieberstein, J., Weihusen, A., Zidowitz, S., Moltz, J.H., Preusser, T., 2010. State of the art in computer-assisted planning, intervention, and assessment of liver-tumor ablation. Critical Reviews™ in Biomedical Engineering 38 (1).
Schumann, C., Rieder, C., Haase, S., Hahn, H., Preusser, T., 2013. Interactive access path exploration for planning of needle-based interventions. Roboter-Assistenten werden sensitiv. 103.
Schumann, C., Rieder, C., Haase, S., Teichert, K., Süss, P., Isfort, P., Bruners, P., Preusser, T., 2015. Interactive multi-criteria planning for radiofrequency ablation. Int. J. Comput. Assist. Radiol. Surg. 10 (6), 879–889.
Scorza, D., Amoroso, G., Cortés, C., Artetxe, A., Bertelsen, Á., Rizzi, M., Castana, L., De Momi, E., Cardinale, F., Kabongo, L., 2018. Experience-based SEEG planning: from retrospective data to automated electrode trajectories suggestions. Healthc. Technol. Lett. 5 (5), 167–171.
Scorza, D., De Momi, E., Plaino, L., Amoroso, G., Arnulfo, G., Narizzano, M., Kabongo, L., Cardinale, F., 2017. Retrospective evaluation and SEEG trajectory analysis for interactive multi-trajectory planner assistant. Int. J. Comput. Assist. Radiol. Surg. 12 (10), 1727–1738.
Scorza, D., Moccia, S., De Luca, G., Plaino, L., Cardinale, F., Mattos, L.S., Kabongo, L., De Momi, E., 2017. Safe electrode trajectory planning in SEEG via MIP-based vessel segmentation. In: Medical Imaging 2017: Image-Guided Procedures, Robotic Interventions, and Modeling, 10135. International Society for Optics and Photonics, p. 101352C.
Seitel, A., Engel, M., Sommer, C.M., Radeleff, B.A., Essert-Villard, C., Baegert, C., Fangerau, M., Fritzsche, K.H., Yung, K., Meinzer, H.-P., et al., 2011. Computer-assisted trajectory planning for percutaneous needle insertions. Med. Phys. 38 (6Part1), 3246–3259.
Sethian, J.A., 1999. Fast marching methods. SIAM Rev. 41 (2), 199–235.
Shamir, R.R., Horn, M., Blum, T., Mehrkens, J., Shoshan, Y., Joskowicz, L., Navab, N., 2011. Trajectory planning with augmented reality for improved risk assessment in image-guided keyhole neurosurgery. In: 2011 IEEE International Symposium on Biomedical Imaging: From Nano to Macro. IEEE, pp. 1873–1876.
Shamir, R.R., Joskowicz, L., Antiga, L., Foroni, R.I., Shoshan, Y., 2010. Trajectory planning method for reduced patient risk in image-guided neurosurgery: concept and preliminary results. In: Medical Imaging 2010: Visualization, Image-Guided Procedures, and Modeling, 7625. International Society for Optics and Photonics, p. 76250I.
Shamir, R.R., Joskowicz, L., Tamir, I., Dabool, E., Pertman, L., Ben-Ami, A., Shoshan, Y., 2012. Reduced risk trajectory planning in image-guided keyhole neurosurgery. Med. Phys. 39 (5), 2885–2895.
Shamir, R.R., Tamir, I., Dabool, E., Joskowicz, L., Shoshan, Y., 2010. A method for planning safe trajectories in image-guided keyhole neurosurgery. In: International Conference on Medical Image Computing and Computer-Assisted Intervention. Springer, pp. 457–464.
Solitro, G.F., Amirouche, F., 2016. Innovative approach in the development of computer assisted algorithm for spine pedicle screw placement. Medical engineering & physics 38 (4), 354–365.
Sparks, R., Vakharia, V., Rodionov, R., Vos, S.B., Diehl, B., Wehner, T., Miserocchi, A., McEvoy, A.W., Duncan, J.S., Ourselin, S., 2017. Anatomy-driven multiple trajectory planning (ADMTP) of intracranial electrodes for epilepsy surgery. Int. J. Comput. Assist. Radiol. Surg. 12 (8), 1245–1255.
Sparks, R., Zombori, G., Rodionov, R., Nowell, M., Vos, S.B., Zuluaga, M.A., Diehl, B., Wehner, T., Miserocchi, A., McEvoy, A.W., et al., 2017. Automated multiple trajectory planning algorithm for the placement of stereo-electroencephalography (SEEG) electrodes in epilepsy treatment. Int. J. Comput. Assist. Radiol. Surg. 12 (1), 123–136.
Talairach, J., Bancaud, J., 1973. Stereotaxic Approach to Epilepsy. In: Progress in neurological surgery, 5. Karger Publishers, pp. 297–354.
Tanaka, D., Shimada, K., Rossi, M.R., Rabin, Y., 2008. Computerized planning of prostate cryosurgery with pullback operation. Computer Aided Surgery 13 (1), 1–13.
Tanaka, D., Shimada, K., Rossi, M.R., Rabin, Y., 2008. Cryosurgery planning using bubble packing in 3d. Comput. Methods Biomech. Biomed. Engin. 11 (2), 113–121.
Teichert, K., 2014. A hyperboxing pareto approximation method applied to radiofrequency ablation treatment planning. Fraunhofer-Verlag.
Tisch, S., Zrinzo, L., Limousin, P., Bhatia, K.P., Quinn, N., Ashkan, K., Hariz, M., 2007. Effect of electrode contact location on clinical efficacy of pallidal deep brain stimulation in primary generalised dystonia. Journal of Neurology, Neurosurgery & Psychiatry 78 (12), 1314–1319.
Trope, M., Shamir, R.R., Joskowicz, L., Medress, Z., Rosenthal, G., Mayer, A., Levin, N., Bick, A., Shoshan, Y., 2015. The role of automatic computer-aided surgical trajectory planning in improving the expected safety of stereotactic neurosurgery. Int. J. Comput. Assist. Radiol. Surg. 10 (7), 1127–1140.
Vakharia, V.N., Sparks, R., Li, K., O'Keeffe, A.G., Miserocchi, A., McEvoy, A.W., Sperling, M.R., Sharan, A., Ourselin, S., Duncan, J.S., et al., 2018. Automated trajectory planning for laser interstitial thermal therapy in mesial temporal lobe epilepsy. Epilepsia 59 (4), 814–824.
Vakharia, V.N., Sparks, R., Miserocchi, A., Vos, S.B., O'Keeffe, A., Rodionov, R., McEvoy, A.W., Ourselin, S., Duncan, J.S., 2019. Computer-assisted planning for stereoelectroencephalography (SEEG). Neurotherapeutics doi:10.1007/s13311-019-00774-9.
Vakharia, V.N., Sparks, R., Rodionov, R., Vos, S.B., Dorfer, C., Miller, J., Nilsson, D., Tisdall, M., Wolfsberger, S., McEvoy, A.W., et al., 2018. Computer-assisted planning for the insertion of stereoelectroencephalography electrodes for the investigation of drug-resistant focal epilepsy: an external validation study. J. Neurosurg. 130 (2), 601–610.

Vakharia, V.N., Sparks, R.E., Li, K., O'Keeffe, A.G., Pérez-García, F., França, L.G., Ko, A.L., Wu, C., Aronson, J.P., Youngerman, B.E., et al., 2019. Multicenter validation of automated trajectories for selective laser amygdalohippocampectomy. Epilepsia.

Van Beers, W., Kleijnen, J.P., 2004. Kriging interpolation in simulation: a survey. In: Proceedings of the 36th conference on Winter simulation. Winter Simulation Conference, pp. 113–121.

Vijayan, R., De Silva, T., Han, R., Zhang, X., Uneri, A., Doerr, S., Ketcha, M.D., Perdomo-Pantoja, A., Theodore, N., Siewerdsen, J.H., 2019. Automatic pedicle screw planning using atlas-based registration of anatomy and reference trajectories. Physics in Medicine & Biology.

Villard, C., Baegert, C., Schreck, P., Soler, L., Gangi, A., 2005. Optimal trajectories computation within regions of interest for hepatic RFA planning. In: International Conference on Medical Image Computing and Computer-Assisted Intervention. Springer, pp. 49–56.

Villard, C., Soler, L., Gangi, A., Mutter, D., Marescaux, J., 2004. Toward realistic radiofrequency ablation of hepatic tumors 3D simulation and planning. In: Medical Imaging 2004: Visualization, Image-Guided Procedures, and Display, 5367. International Society for Optics and Photonics, pp. 586–595.

Villard, C., Soler, L., Papier, N., Agnus, V., Thery, S., Gangi, A., Mutter, D., Marescaux, J., 2003. Virtual radiofrequency ablation of liver tumors. In: International Symposium on Surgery Simulation and Soft Tissue Modeling. Springer, pp. 366–374.

Wicker, R., Tedla, B., 2004. Automatic determination of pedicle screw size, length, and trajectory from patient data. In: The 26th Annual International Conference of the IEEE Engineering in Medicine and Biology Society, 1. IEEE, pp. 1487–1490.

Wimmer, W., Venail, F., Williamson, T., Akkari, M., Gerber, N., Weber, S., Caversaccio, M., Uziel, A., Bell, B., 2014. Semiautomatic cochleostomy target and insertion trajectory planning for minimally invasive cochlear implantation. Biomed. Res. Int. 2014.

Xiaozhao, C., Jinfeng, H., Baolin, M., Chongnan, Y., Yan, K., 2016. A method of lumbar pedicle screw placement optimization applied to guidance techniques. Computer Assisted Surgery 21 (sup1), 142–147.

Yang, L., Wen, R., Qin, J., Chui, C.-K., Lim, K.-B., Chang, S.K.-Y., 2010. A robotic system for overlapping radiofrequency ablation in large tumor treatment. IEEE/ASME Trans. Mechatron. 15 (6), 887–897.

Yaniv, Z., Cheng, P., Wilson, E., Popa, T., Lindisch, D., Campos-Nanez, E., Abeledo, H., Watson, V., Cleary, K., Banovac, F., 2009. Needle-based interventions with the image-guided surgery toolkit (IGSTK): from phantoms to clinical trials. IEEE Trans. Biomed. Eng. 57 (4), 922–933.

Yu, J., Liang, P., Yu, X., Liu, F., Chen, L., Wang, Y., 2011. A comparison of microwave ablation and bipolar radiofrequency ablation both with an internally cooled probe: results in ex vivo and in vivo porcine livers. Eur. J. Radiol. 79 (1), 124–130.

Yushkevich, P.A., Piven, J., Hazlett, H.C., Smith, R.G., Ho, S., Gee, J.C., Gerig, G., 2006. User-guided 3d active contour segmentation of anatomical structures: significantly improved efficiency and reliability. Neuroimage 31 (3), 1116–1128.

Zelmann, R., Bériault, S., Marinho, M., Mok, K., Hall, J.A., Guizard, N., Haegelen, C., Olivier, A., Pike, G.B., Collins, D.L., 2015. Improving recorded volume in mesial temporal lobe by optimizing stereotactic intracranial electrode implantation planning. Int. J. Comput. Assist. Radiol. Surg. 10 (10), 1599–1615.

Zelmann, R., Beriault, S., Mok, K., Haegelen, C., Hall, J., Pike, G.B., Olivier, A., Collins, D.L., 2013. Automatic optimization of depth electrode trajectory planning. In: Workshop on Clinical Image-Based Procedures. Springer, pp. 99–107.

Zhai, W., Xu, J., Zhao, Y., Song, Y., Sheng, L., Jia, P., 2008. Preoperative surgery planning for percutaneous hepatic microwave ablation. In: International Conference on Medical Image Computing and Computer-Assisted Intervention. Springer, pp. 569–577.

Zhang, Q., Li, M., Qi, X., Hu, Y., Sun, Y., Yu, G., 2018. 3D path planning for anterior spinal surgery based on CT images and reinforcement learning. In: 2018 IEEE International Conference on Cyborg and Bionic Systems (CBS). IEEE, pp. 317–321.

Zhang, R., Wu, S., Wu, W., Gao, H., Zhou, Z., 2019. Computer-assisted needle trajectory planning and mathematical modeling for liver tumor thermal ablation: a review. MATHEMATICAL BIOSCIENCES AND ENGINEERING 16 (5), 4846–4872.

Zombori, G., Rodionov, R., Nowell, M., Zuluaga, M.A., Clarkson, M.J., Micallef, C., Diehl, B., Wehner, T., Miserochi, A., McEvoy, A.W., et al., 2014. A computer assisted planning system for the placement of SEEG electrodes in the treatment of epilepsy. In: International Conference on Information Processing in Computer-Assisted Interventions. Springer, pp. 118–127.

Zuluaga, M.A., Rodionov, R., Nowell, M., Achhala, S., Zombori, G., Mendelson, A.F., Cardoso, M.J., Miserocchi, A., McEvoy, A.W., Duncan, J.S., et al., 2015. Stability, structure and scale: improvements in multi-modal vessel extraction for SEEG trajectory planning. Int. J. Comput. Assist. Radiol. Surg. 10 (8), 1227–1237.